Synthesis chemistry and application development of periodic mesoporous organosilicas

Hou-Sheng Xia · Chun-Hui (Clayton) Zhou · Dong Shen Tong · Chun Xiang Lin

Abstract This paper provides a comprehensive and critical overview of recent advances in synthesis chemistry and application development of periodic mesoporous organosilicas (PMOs). A number of organic bridge-bonded functional and multifunctional PMOs with inorganic–organic hybridized framework have been synthesized from varieties of precursors. The syntheses of a series of PMOs have been accomplished typically by resorting to the co-condensation of the mixed precursors of tetraalkoxysilane and bridged organosiloxane, bridged organosiloxane with terminal organosiloxane, or the co-condensation of multiple bridged organosiloxane. The choice of precursors depends on the desired location of organic groups which can be either on the surface or within the pore wall in resulting PMOs. Besides precursors, synthesis conditions evidently play an important role in the formation, morphologies and pore structure of PMOs. Recent advances show that the morphologies and mesopores of PMOs can be adjusted by changing the synthetic parameters such as template, additives, pH value, and temperature. The PMOs with tunable composition, morphology and even-distributed hydrophobic organic groups in the framework endow such periodic mesoporous hybrids with great potentials in the fields of catalysis, environmental remediation, biology, pharmacy, analytical chemistry and microelectronics. The synthesis chemistry of PMOs and application development would particularly and continuously appeal to the researchers in chemistry and materials science in future.

Keywords Periodic mesoporous organosilicas · Bridged organosiloxane · Porous materials · Synthesis chemistry · Hybrid · Co-condensation · Template · Catalytic materials · Review

H.-S. Xia · Chun-Hui (Clayton)Zhou (✉) · D. S. Tong
Research Group for Advanced Materials & Sustainable Catalysis (AMSC), ZJUT & RenHeng R&D Center for Advanced Clay-Based Materials (CCM), Institute of Catalytic Materials (ICM), Zhejiang University of Technology (ZJUT), Shang Tang Road, Hangzhou, Zhejiang 310032, People's Republic of China
e-mail: catalysis8@yahoo.com.cn; clay@zjut.edu.cn

C. X. Lin
School of Engineering, ARC Centre of Excellence for Functional Nanomaterials, The Australian Institute for Bioengineering and Nanotechnology, The University of Queensland, St. Lucia, QLD 4072, Australia

1 Introduction

The invention of novel mesoporous materials provides a powerful stimulus to scientific and technological advancement in catalysis, adsorption and separation, biomaterials, and nano-scaled electronic, optical, magnetic devices. A number of mesoporous silica-based materials with pore size in the range of 2–50 nm are prepared generally through template structure-directed synthesis strategies. Some typical materials are M41S [1], FSM-16 [2], SBA-n [3, 4], HMS [5], MSU-n [6, 7] and KIT-1 [8]. Traditionally, microporous zeolites and their analogs (Scheme 1a) are synthesized by using single small organic molecule as template, and consequently the pore sizes of the resulting materials are mainly distributed in the range of micropore less than 2 nm. Such small pores limit the applications of microporous zeolites in the cases of larger molecules involved. Therefore, in this aspect the advent of mesoporous materials casts new light on the adsorption and transformation of large organic molecules.

The extension of mesoporous silica to mesoporous inorganic–organic hybrid materials, which contain organic groups as an integral part of the structure, expands much

Scheme 1 The schematic drawings of three kinds of silica-containing materials. **a** Inorganic silica or Al-Si zeolite material. **b** Grafting organosilicas. **c** Periodic mesoporous organosilicas

(a)

Al or O atom

(b)

Terminal organic gruop

(c)

Bridging organic gruop
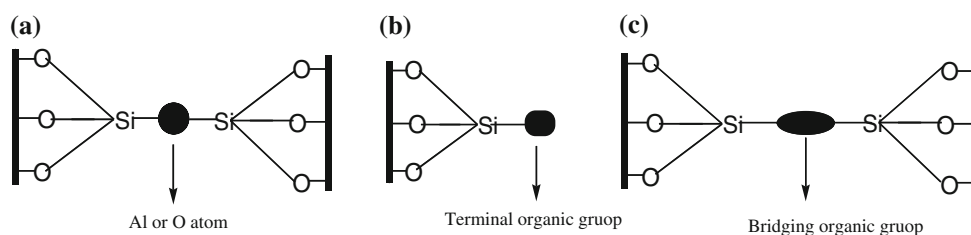
the potentials of such mesoporous materials to be used as catalysts, adsorbents, trapping agents, stationary phases in chromatography and chemical sensors [9–12]. Earlier, such porous organosilicas with terminal organic groups (Scheme 1b) were prepared either by grafting organic group onto the channel wall using the reactivity of the silanol groups in the material or by template-directed co-condensation of tetraethoxysilane (TEOS) and organotrialkoxysilanes [13, 14]. Compared with non-functionalized inorganic mesoporous materials, most of surface organic-functionalized mesoporous materials exhibit disordered structures and scattered pore-size distribution.

By combining the methodology of the use of bridged silsesquioxanes as precursors with the supramolecular templating approach, a series of novel periodic mesoporous organosilica hybrids are successfully created [15, 16]. Not only does this class of organic–inorganic hybrids possess homogeneous distribution of organic fragments and inorganic oxide within the framework, instead of surface-grafted organic groups, but also exhibits uniform mesopores with even more ordered structure. Such materials are termed as periodic mesoporous organosilicas (PMOs). As shown in Scheme 1c, PMOs are quite different from the previous surface organic-functionalized mesoporous materials and amorphous organic–inorganic hybrid materials. Table 1 gives a classification scheme of mesoporous materials according to the position and kinds of organic groups in the matrix. Among those materials, only the class III, IV, V hybrids are regarded as PMOs in word and deed which are reviewed hereafter [17].

In general, PMOs are synthesized by hydrolysis and oligomerization of bridged silsesquioxane in the presence of various structure-directing agents (SDA) such as ionic

surfactants, oligomeric surfactants, and nonionic block copolymers. The synthesis parameters may not only allow to tailor such physical properties of PMOs as density, thermal and mechanical stability, hydrophobicity, hardness, electrochemical properties, fracture toughness, but also permit the agile chemical modification of framework by the change of the organic bridge-bonded moiety. The stoichiometric incorporation of organic groups in the silica framework becomes feasible. The multiplicity of organic bridge-bonded groups endows PMOs with novel properties associated with both organic and inorganic materials. Moreover, after removal of template by post-treatment, the void space is left unoccupied. The open mesopores with much higher loading and homogeneous distribution of organic functional group in the framework have greatly improved the accessibility of larger molecules to functional sites. As a result, PMOs become a class of materials with much promising potentials in such many fields as nanocluster synthesis, ceramics, shape-selective adsorption and catalysis, optoelectronic materials, low-k microelectronic packaging materials, purification, chromatography, nanoreactors and sensing devices as well as immobilization and encapsulation of biomolecules [17–27].

2 The synthesis of periodic mesoporous organosilicas

The synthesis procedure of PMOs is similar to that of mesoporous silicas (MPS), namely, hydrothermally surfactant-mediated sol–gel methods. In other words, PMOs are synthesized through hydrolytic polycondensation of one or more kinds of silsesquioxane precursors, including (1) bis(trialkoxysilyl)organics $(RO)_3Si\ R'Si(OR)_3$ {R = $-CH_3$

Table 1 Classification of mesoporous inorganic materials and periodic mesoporous organosilicas

Class	Description	Structure unit	Example
I	Mesoporous silica	$O_3Si–O–SiO_3$	MCM-41, SBA, HMS
II	Terminally bonded monofunctional	T- $O_2Si–O–SiO_3$	Vinyl-containing MCM-41
III	Bridge-bonded monofunctional	$O_3Si–B–SiO_3$	Ethane-PMOs, Benzene-PMOs
IV	Bridge-bonded bifunctional	$O_3Si–B_1–SiO_2–Si–B_2–SiO_3$	PMOs containing both ethane and benzene groups.
V	Mixed bridge-bonded and terminally-bonded	T- $O_2Si–O–Si–B–SiO_3$	Ethane-PMOs with terminal groups such as thiol, sulfonic acid

T represents a terminal organic groups such as $–SO_3H$, $–CH=CH_2$, B represents a bridging organic group such as $–CH=CH–$, $–C_6H_4–$. B_1 is different from B_2

or –C_2H_5, R′ ranging from simple alkane chains to aromatic groups to very large organometallic complexes.} [28] or (2) cyclic siliquioxane precursor, for instance, ([(EtO)$_2$SiCH$_2$]$_3$) [29] in the presence/absence of tetraalkoxysilane under certain reaction conditions such as template, pH value, temperature, pressure, ageing time and so on. The template can be removed by solvent-extraction, ion-exchange or moderate calcination [30]. With different choice of organic bridge-bonded precursors, surfactant templates, and reaction conditions, a great variety of PMOs with various properties can be obtained. Moreover, PMOs with two or more organic functionalities can be achieved by such strategies as (i) co-condensation of a bridged organosiloxane precursor with a terminal organosiloxane precursor, and (ii) co-condensation of multiple bridged organosiloxane precursors.

2.1 Synthesis of PMOs with unitary organic bridging groups

PMOs with unitary bridged organic groups can be synthesized by merely using bridged silsesquioxane as precursor (Scheme 2a). This method can yield PMOs with much higher loading of organic groups in the framework. However, this precursor sometimes leads to materials with a lower degree of formation of channels because some organic functional moieties, particularly organic group with complex chemical structures, tend to perturb the micellar template structure. To address this problem, attempts were made to synthesize such PMOs by means of co-condensation of TEOS or tetramethylorthosilicate (TMOS) and bridged silsesquioxane (Scheme 2b). Nevertheless, the maximum incorporation of bridged silsesquioxane is limited around 20–25 mol.%, owing to the addition of TEOS required for full condensation into the rigid and ordered framework.

So far, PMOs with such organic bridged parts as methane [31], ethane [32, 33], benzene [34–36], toluene, 2,5-dimethylbenzene [37], thiophene [38], p-xylene [39], biphenyl [40],

1,3,5-benzene [41], interconnected [Si(CH$_2$)]$_3$ rings [29], 4-phenylether, 4-phenylsulfide units [42], and isocyanurate rings [43] have been reported. These PMOs can be divided into three categories, i.e., alkyl (alkane, alkene, alkyne) group-bridged PMOs, aromatic group-bridged PMOs and heterocycle group-bridged PMOs, in terms of their bridging functional groups (Table 2).

2.1.1 PMOs with alkyl groups

The overwhelming majority of PMOs deals with the synthesis of mesoporous alkyl-silica, possibly because bis-(trialkoxylsilyl)alkyl as silsesquioxane precursor is readily available [44]. Many organosilane precursors with various aliphatic chains can be used for the synthesis of amorphous porous hybrid materials before, but just certain organosilane with short and flexible aliphatic chains, such as bis-silylated ethane, ethylene, and methylene, are normally chosen as precursors to synthesize their corresponding alkyl-PMOs. Among those, bis(trimethoxysilyl)ethane (BTME) and bis(triethoxysilyl)ethane (BTESE) are two of the most commonly used precursors because of their similarity in hydrolysis and condensation behaviors to those of TEOS, which is frequently used in the synthesis of MPS materials. PMOs derived from the former two precursors and TEOS are mostly synthesized by using similar experimental conditions to their pure silica counterparts [28, 45]. Although BTESE looks equivalent to BTME, because BTME and BTESE have different silyl groups, namely, methyl and ethyl, respectively, hydrolysis of BTESE is slower than that of BTME owing to steric hindrance at the larger ethoxide moieties and reduced solvation of resulting ethanol. This also takes place in TEOS and TMOS system [46, 47]. Because faster hydrolysis of organosilica precursors is favorable, PMOs synthesized by the hydrolysis and condensation of BTME have more ordered structure than those obtained from BTESE [48].
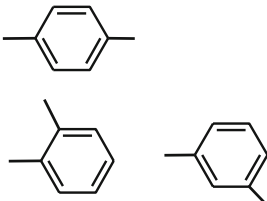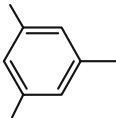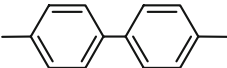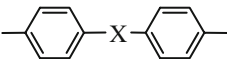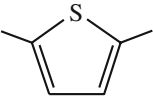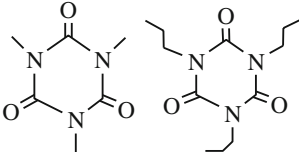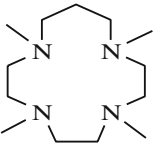
Regarding further fuctionalization in the case of PMOs from BTESE, the ethane linkers offer less application
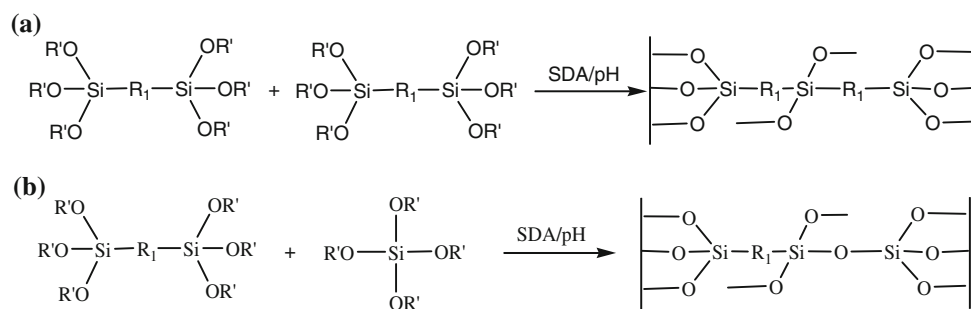
Scheme 2 PMOs synthesized from one kind of bridged silsesquioxane (SDA: structure-directing agents). **a** PMOs synthesized by hydrolysis and oligomerization of bridged silsesquioxane in presence of SDA. **b** PMOs synthesized by co-condensation of bridged silsesquioxane and tetraalkylorthosilicate in presence of SDA

Table 2 The classification of monofunctional PMOs according to the type of polysilsesquioxane precursor

Type	Si precursor	Bridged groups	Particular properties
Alkyl group-bridged PMOs	Bis(triethoxysilyl)methane (BTM)	$—CH_2—$	Easily transform from bridging moieties to terminal groups
	1,2-bis(trimethoxysilyl)ethane (BTME)	$—CH_2—CH_2—$	Most frequently used to synthesize PMOs
	1,2-bis(trimethoxysilyl) ethylene (BTMNE)	$—C{=}C—$ with H	A wide range of opportunities for further surface modifications based on olefin chemistry
Aromatic group-bridged PMOs	1,i-bis(triethoxysilyl)benzene (BTEB) i = 4,2,3		Exhibit both long- and short-range order for π–π intermolecular interactions between aromatic rings
	1,3,5-(triethoxysilyl)benzene		More stable due to their linkages to three siloxanes bound to three silicon atoms both as a functional group and a cross-linker
	4,4′bis(triethoxysilyl)biphenyl		The periodicity is larger than the periodicity observed in phenylene-bridged material
	Bis-4-(triethoxysilyl)phenyl-ether/sulfide		PMOs with ''ligand channels'' and might be environmentally useful for sequestering toxic heavy metal ion
Heterocycle group-bridged PMOs	2,5-bis(triethoxysilyl)-thiophene		High (maximum) concentration of coordination sites within the pores, good for electrochemical applications
	Tris[3-(trimethoxysilyl)propyl]-isocyanurate		Isocyanurate ring is integrated with three trimethoxysilyl groups through flexible propyl chains, so many groups were introduced and structural ordering was rather high
	1,4,8,11-tetraazacyclotetra-decanetrimethoxysilane		Remarkable binding ability towards transition metal cations. But the introduced group was little and structural ordering was rather poor

because it merely contains saturated C–C bonds. Comparatively, periodic mesoporous ethylenesilica may offer a wide range of opportunities for further surface modification based on the unsaturated bonds in olefin in the framework [49]. Bridge-bonded ethene groups can be directly integrated into the framework of the resulting stable PMOs from a synthesis system of bis(triethoxysilyl)ethene (BTSENE), TEOS, SAD, NH$_4$OH and H$_2$O [16]. Bromination of the ethene groups was conducted to test the chemical accessibility of ethene groups in ethene-PMOs. These results showed that ethene groups incorporated into the channel walls are accessible for chemical reaction and modification. Nonetheless, chemical analysis of the brominated ethene-PMOs indicated that it contained less bromine than the amount expected for 100% bromination. The results showed that while some ethene groups ($\sim$10%) were brominated, others reacted with the solvent of CH$_2$Cl$_2$/Br$_2$ to form ethane bridges. Compared PMOs containing ethene groups with mesoporous silica tethered vinyl groups inside the channels, the bridging ethene groups housed within the silica framework and attached to two electron-withdrawing O$_3$Si– framework moieties, is less active than the terminal vinyl groups located in the channel space and attached to one O$_3$Si– group [50].

Ethylene-bridged mesoporous organosilica spheres were successfully synthesized via surfactant-mediated assembly of BTSENE [51]. The ordering of the ethylene-bridged mesoporous sphere morphology can be controlled by the basicity of the synthesis media. Such mesoporous spheres exhibit molecular-scale periodicity due to the π–π interaction between ethylene groups and good mesostructural ordering in the organosilica framework. The readily functionalized organic groups and the morphology of relatively monodispersed sphere morphology with tunable size lead to the flexibility of ethylene-bridged mesoporous materials.

Since methylene is a simplest organic group isoelectronic with oxygen, methane-bridged PMOs are conceived as ideal model materials for theoretic investigation [52]. Asefa et al. [31] have prepared PMOs with bridging methylene spacers incorporated into the wall of hexagonally close packed channel using bis(triethoxysilyl)methane (BTM) as organosilica precursor. This material exhibits enhanced chemical and thermal stability up to 700 °C in air. The so-called channel metamorphosis of PMOs may take place so that PMOs with organosilica channels containing bridging organic moieties are chemically transformed to PMOs having terminally bonded organic groups located in the mesopores.

By using cyclic silsesquioxane precursor of 1,3,5-tris[diethoxysila]-cyclohexane [{SiCH$_2$(OEt)$_2$}$_3$], PMOs with far higher organic loading can be achieved because each silicon tetrahedral center is bound to two methylene groups to give an approximate composition of SiOCH$_2$ [29].

It was demonstrated that such cyclic silsesquioxane precursors can be co-assembled with a surfactant mesophase to yield PMOs in either powder or oriented film morphology. To improve the complexity and the hierarchical order of the channel wall, PMOs with high organic group content were synthesized from precursors of silsesquioxane [{[(EtO)$_2$SiCH$_2$]$_2$[(EtO)$_2$SiCH]}$_2${(CH$_2$)$_3$}}] with trimethylene-bridged 3-rings, in which two cyclic building blocks are bridged by an organic group. The PMOs are successfully made from these precursors through NaCl-assisted acid-catalyzed self-assembly with the triblock copolyether P123 as template [53]. The integrity of trimethylene-bridged 3-ring building block is kept intact in the channel wall of the well-ordered PMOs. These PMOs were found thermally stable with no mass loss up to 400 °C in a N$_2$ atmosphere.

2.1.2 PMOs with aryl groups

The PMOs can be self-organized through diversiform interactions, such as van der Waals type [54], hydrogen-bonding [55, 56], π–π-stacking [57] and hydrophobic–hydrophilic [58] interactions, promoted by groups within the organic bridged fragment. Organosilicas with molecular periodicity of organic aryl units have been synthesized by surfactant-templated self-organization of bissilylated organic monomers containing rigid and symmetrical aromatic groups such as phenylene, and biphenylene. Besides the assistance of surfactant, the formation of such PMOs can also be aided by π–π intermolecular interactions between aromatic rings and hydrogen bonding between C-SiOH groups, leading to preferential alignment of the organic bridges in the organosilica network [59]. Analogous interactions can be exploited in the synthesis of a variety of hierarchically ordered materials with hybrid organo-metal oxides [39].

Yoshina-Ishii et al. [52] used 1,4-bis(triethoxysilyl)benzene (BTEB) as precursor to prepare PMOs with bridging aromatic group. The resulting organosilica shows only a small amount of Si–C bond cleavage and exhibits a good hexagonal mesoporous phase. Inagaki et al. [60] discovered that PMOs synthesized from BTEB under basic conditions in the presence of octadecyltrimethylammonium chloride (C$_{18}$TMACl) exhibit both long- and short-range order and the hexagonal array of mesopores and crystal-like pore walls possess structural periodicity in the wall along the channel direction with a spacing of 7.6 Å. However, such self-assembly process suffers from challenge when "flexible" methylene spacers are added to "rigid" aromatic bridged silsesquioxane precursors. The corresponding PMOs were tentatively prepared by polymerizing phenylene bridged silsesquioxane precursors containing an incremental increase in methylene spacers [1,4-(CH$_2$)$_n$C$_6$H$_4$ (n = 0–2)]. But these materials lack long-range order [61].

The biphenylene-bridged PMOs was also synthesized using 4, 4′-bis(triethoxysilyl)biphenyl [$(C_2H_5O)_3Si$–$(C_6H_4)_2$–$Si(OC_2H_5)_3$] precursor in basic medium in the presence of C_{18}TMACl surfactant [40], and the periodicity of 11.6 Å is larger than the periodicity of 7.6 Å observed in phenylene-bridged mesoporous material. This is attributed to the increased length of biphenylene group compared to that of phenylene group. Recently, Yang and Sayari [62] have synthesized PMOs from biphenylene bridged polysilsesquioxane precursor with Pluronic P123 as SDA under acidic condition. Characterization results suggested that these PMOs have wormhole mesoporous structure with molecular scale order of biphenyl species in a layered structure within the pore wall. In addition to the higher surface area, these mesoporous organosilicas under acidic condition have larger pore volume than the PMOs prepared under basic condition.

Besides the symmetrically linear bridged organosilane precursors, nonlinear symmetric bridged organosilane precursors can also be used to synthesize PMOs with mesoscopically ordered pores and molecularly ordered pore walls [63]. For instance, 1,4-bis(triethoxysilyl)benzene (1,4-BTEB) has a linear rigid rod-like geometry whereas the other derivatives, 1,3-bis(triethoxysilyl)benzene(1,3-BTEB) and 1,2-bis(triethoxysilyl) benzene (1,2-BTEB) organosilica precursors, have the nonlinear symmetric structure. Both precursors were successfully used to synthesize their corresponding PMOs. Interestingly, there is little difference in the molecular scale periodicities of PMOs synthesized from 1,4-BTEB and 1,3-BTEB precursors, respectively, although they have different molecular geometry.

Unlike bivalent oxygen atoms as linkers between silicon atoms in most porous silica materials, however, organic functional groups can be made to bind more than two silicon atoms and thus they can be used not only as functional groups but also as cross-linkers in the structure to form rigid organic–inorganic frameworks. Kuroki et al. [41] have demonstrated this possibility by using a 1,3,5-benzene group bound to three silicon atoms both as a functional group and as a cross-linker. As a result, these aromatic PMOs contain benzene functional groups symmetrically integrated with three silicon atoms in the organosilica mesoporous framework. The functional aromatic moieties undergoes sequential thermal transformation from three to two and then to one point attachment within the framework upon continuous pyrolysis under air and eventually the materials turn into periodic mesoporous silica devoid of aromatic groups at high temperature and longer pyrolysis time. The benzene rings in aromatic PMOs, for example, 1,3,5-benzene PMOs, are found more stable due to their linkages to two and three siloxanes, respectively, compared to singular alkene-containing PMOs. However, 1,3,5-benzene PMOs have no molecular-scale periodicity in the pore

wall because the acidic condition would not be appropriate to orient phenylene groups.

2.1.3 PMOs with heterocycle groups

The synthesis of PMOs with heterocycle groups are more challenging compared to the synthesis of PMOs with short aliphatic chains and symmetrical aryl bridging groups. Firstly, it is difficult to prepare organosilane precursors containing heterocycle groups. Secondly, the heterocycle groups incorporated in the framework are unstable and thus are easily eliminated during subsequent treatment such as template removal by solvent extraction or calcination [64]. Thirdly, large and complex organic groups usually have high hydrophobic, steric influence and electronic effect, which indirectly influence the interaction between organosilane precursors and template. Numerous attempts have been made to overcome this roadblock. Among them are incorporation of larger organic spacers such as thiophene, tetraazacyclotetradecane, isocyanurate, phenyl ether and chiral groups into PMOs [65].

Due to the very high concentration of coordination sites within the pores, thiophene-PMOs are of particular interest for applications in electrochemical materials or functionalized materials for hosting different types of nanoclusters. To obtain ordered PMOs containing thiophene in an aqueous synthesis medium, earlier the thiophene PMOs were synthesized by hydrolytic polycondensation of 2,5-bis(triethoxysilyl) thiophene using low molecular weight surfactants such as cetylpyridinium chloride (CPCl) [52]. However, the resulting products exhibited lower structural order accompanied by small pores. Therefore, another synthesis method has been attempted and therein cetylpyridinium chloride was replaced by triblock copolymer (Pluronic P123) as SDA [66]. Then the corresponding thiophene-PMOs not only have larger pore size but also demonstrate thermal stability up to 400 °C in air which is essential for application at elevated temperature.

1,4,8,11-Tetraazacyclotetradecane (cyclam) have remarkable binding ability towards transition metal cations [67–69]. The direct synthesis of PMOs containing cyclam groups has been achieved by hydrolysis and polycondensation of cyclam group bridged organosilica precursor and TEOS in the presence of SDA [70]. The immobilization of this large chelating group allows the grafting of functional groups inside channel pores. Furthermore, the textural characteristics of these materials with narrow pore size distribution can be modified by changing the synthesis condition. Nevertheless, the percentage of introduced groups was small and structural ordering was rather poor.

PMOs with isocyanurate bridging groups in cage-like mesopores are synthesized by co-condensation of TEOS and tris[3-(trimethoxysilyl)propyl]isocyanurate in the

presence of Pluronic P123 under acidic condition [43, 71]. Due to the fact that the isocyanurate ring is integrated with three trimethoxysilyl groups through flexible propyl chains, 75–90% of tris[3-(trimethoxysilyl)propyl]isocyanurate relative to the total amount of silica sources was substantially used during synthesis without remarkable loss of their structural ordering. The resulting PMOs have relatively high loading of large heterocyclic isocyanuarte rings (ISC), high total pore volume, and high surface area. In addition, an efficient removal of the polymeric template was achieved by heating of the extracted ISC-PMOs in nitrogen at 315 °C for 4 h and the treatment can improve the total pore volume, and high surface area of the resulting material.

The 4-phenyl ether bridge was previously used to form a soluble ladder-like polyvinylsiloxane from 4,4′-bis(vinyldimethyloxysilyl)phenyl ether with a maximum of two siloxane bonds per silicon center [72]. Recently, PMOs were prepared by mixing thioether bridged silsesquioxane with TEOS as a network former [73]. The PMOs with 4-phenyl ether and 4-phenyl sulfide bridge-bonded silsesquioxanes in which oxygen or sulfur atoms form hinge groups between two 4-phenyl silsesquioxane rings, integrated into the pore wall to create ligand channels have been synthesized using inorganic salt-assisted self-assembly with supramolecular polyoxyethylene (10) stearyl ether (Brij 76) as template [42]. The bis-4-(triethoxysilyl)phenyl ether/sulfide precursor containing six condensable Si–O units can yield a more robust and insoluble cross-linked structure. This new class of PMOs with ''ligand channels'' prove environmentally useful for sequestering toxic heavy metals and organic pollutants from waste water and for being as support for heterogeneous catalysts.

Highly ordered PMOs with the 1,4-diureylenebenzene (DUB) moieties incorporated into the framework were synthesized through co-condensation of bissilylated 1,4-diureylenebenzeneand TEOS using triblock copolymer P123 as a SDA in acidic solutions [74, 75]. The maximum amount of such organic groups incorporated into the PMOs reached 10 mol.%. Uniform rod-like morphology of PMOs was obtained accompanied by the increasing organic parts of the PMOs. However, the presence of the excessive DUB fraction in the silica matrix would decrease the mesoscopic order of the PMOs and eventually lead to the collapse of the mesoporous structure. The reason might be interpreted by the intermolecular hydrogen-bonds interactions between the ureylene groups located inside the silica networks.
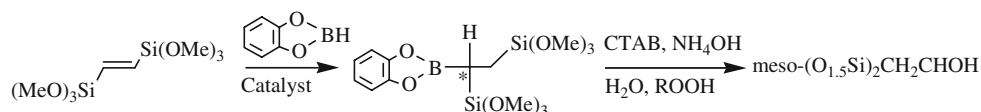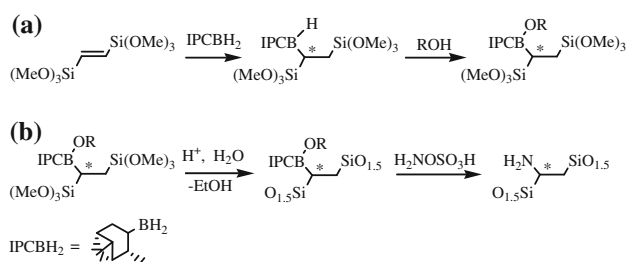
2.1.4 PMOs with chiral groups

Mesoporous chiral organosilicas (ChiMOs) can be theoretically obtained by introducing chiral organic groups into the R bridge between the silicon atoms [76]. The chiral bridging functional groups usually have a complex chemical structure and are difficult to integrate into the silica framework [77]. An alternative way is to add chiral organic groups to the silane groups via long and flexible linkers such as propyl, benzyl group [78]. Moreover, in order to increase the solubility of the large chiral precursor in aqueous solution, co-solvent, for instance, ethanol is needed [79].

Molecules of $(R'O)_3Si–CH_XCH_2–Si(OR')_3$, where X can be any groups except hydrogen, represent an attractive group of chiral PMO precursors because of their small organic group and hydrophilicity. Such kind of chiral precursors can be prepared by the "all-in-one" approach [80]. For instance, an ethylene-bridged precursor was converted into a chiral alcohol by using rhodium(I) catalysts in combination with (R)-(+)-2,2′-bis(diphenylphosphino)- 1,1′-binaphthalene(R-BINAP) as a chiral ligand, as shown in Scheme 3.

Thomas et al. [81] synthesized a chiral precursor by convenient enantioselective hydroboration using (S)-monoisopinocampheylborane on an ethylene-bridged silica precursor. Then chiral PMOs were prepared by condensation with this chiral precursor and TEOS, and then amine-functionalized ChiMOs were ammonolysized by hydroxylamine-O-sulfonic acid (Scheme 4). The so-prepared organosilicas exhibit a tunable functionality and porosity and a very high and accessible surface area.

Besides the chiral precursors, the synthesis of chiral mesostructured silica using a chiral template has also been reported [82, 83]. For instance, a chiral cationic fluorinated surfactant $[CF_3(CF_2)_3SO_2NH(CH_2)_3N^+ (CH_3)_3I^-]$ (FC-4911) and the cationic hydrocarbon surfactant $C_{16}TABr$ were employed as SDA, while BTSENE or BTEB were used as hybrid precursors [84]. The quantity of left-handed particles was almost equal to that of right-handed ones for both ethene-PMOs and benzene-PMOs, thus indicating that it is a racemic mixture. However, the left-to-right-handed ratio was increased to 55/45 by adding a small amount of sodium L-tartrate during the preparation. Such results may suggest that the driving forces for the formation of helical structures come from the addition of fluorinated surfactants. The use of

Scheme 3 Synthesis of PMOs containing chiral alcohol by the "all-in-one" approach. Adapted from [80]. Copyright 2006, with permission from Wiley-VCH

(a)

(b)

Scheme 4 **a** Enantioselective synthesis of chiral PMOs precursors via hydroboration with (S)-isopinocampheylmonoborane. **b** Hydrolysis, condensation, and ammonolysis of the precursor. Adapted from [81]. Copyright 2006, with permission from American Chemical Society

appropriate chiral additives may enhance the enantiopurity of the final products.

2.2 Synthesis of PMOs containing more than one kind of organic groups

PMOs simultaneously containing several kinds of organic groups are more multifunctional. Such PMOs with various organic bridging groups, morphology, and structural symmetry of the porous network are generally synthesized by co-condensation of precursors bearing multiple organic functionalities. These approaches to prepare such PMOs using different bridged silsesquioxanes as co-precursors have broadened the scopes of PMOs and have provided new routes to tailor the properties with more multifunctionality.

2.2.1 PMOs with both bridged and terminal organic groups

PMOs with terminally bonded organic groups in the channels are synthesized by the addition of $RSi(OR)_3$ precursors via direct synthesis or post-synthesis. This method had been often used for surface functionalization and framework modification of inorganic mesoporous materials, yielding the active sites on the surface and near the pore [9, 85]. PMOs with one small bridging group and one surface ligand (cf. Table 1, Class V multifunctional hybrid materials) can be prepared by either post-synthesis grafting [86] or co-condensation. The co-condensation method has several advantages over post-synthesis method, including the simpler synthetic protocols of one-pot reaction, the better control of the loading of organosilanes, and an even distribution of organic groups. Moreover, the fact that the pore surface of PMOs is comparably inert could make post-synthesis grafting difficult. Therefore, PMOs with both bridged and terminal organic groups are usually synthesized by co-condensation of an organosilsesquioxane and an organosilane with/without TEOS (Scheme 5).

Among the various functionalized PMOs, more attractive are those with amino functional groups due to the
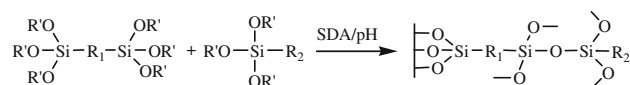
Scheme 5 PMOs synthesized from bridged organosiloxane precursors and terminal organosiloxane precursors

possible versatile application associated with amine chemistry, which include base-catalysis, coupling and immobilization of functional molecules and biomolecules, and adsorption and sequestration of metal ions. The synthesis of amine-functionalized PMOs by co-condensation of BTESE and amino-containing silane has been reported [87]. Unlike TEOS, BTESE mixes well with trialkoxyorganosilane. Burleigh et al. have synthesized a series of amine-functionalized PMOs with various trialkoxyorganosilanes, such as 3-aminopropyltrimethoxysilane, n-(2-aminoethyl)-3-aminopropyl- trimethoxysilane [88], 2-(trimethoxysilylethyl)pyridine, and N-(3-triethoxysilylpropyl)-4,5-dihydroimidazole [89] (Scheme 6). The bridged organosilane allowed a higher loading of the functional groups than mesoporous pure silica materials.

The synthesis of amine-functionalized PMOs can also be achieved by co-condensation of 1,4-bis(triethoxysilyl) benzene (BTEB) and amino-containing silane. Coutinho et al. [90] synthesized functionalized mesoporous benzene silica hybrids containing propylamine, propylethylenediamine, and propyldihydroimidazole by the direct co-condensation of BTEB with (3-aminopropyl)trimethoxysilane, [3-(2-aminoethylamino)-propyl]trimethoxysilane, or N-(3-triethoxysilylpropyl)-4,5-dihydroimidazole. Changing the molar ratio of amino-containing silane brings about a series of nitrogen-containing bifunctional PMOs. As the molar ratio approaches 50%, the pore wall will be mainly composed by amine as well as the bridging benzene, resulting in larger pore materials at the expense of long range order.

For potential use as solid acid catalysts, there has been considerable interest in developing mercapto/sulfonic acid functionalized PMOs [91–94]. The preparation process for most of bridged PMOs with anchored sulfonic acid groups is that thiol-functionalized PMOs are first prepared by co-condensation, followed by oxidation of the thiol group by aqueous H_2O_2 or concentrated HNO_3 (Scheme 7).

Ethane–PMOs bearing the sulfonic acid were first synthesized by using BTME and mercaptopropyltrimethoxysilane (MPTMS) as precursors [95]. Conversion of the mercaptopropyl groups into sulfonic acid moieties is achieved via oxidation using hydrogen peroxide in a methanol–water mixture [94, 96]. The amount of MPTMS varied from 0 to 50 mol.% ($x = 0$–0.5). With increasing amounts of MPTMS, the sulfonic acid functionalized PMOs show increased acidities, but porosity, structural order and oxidation efficiency decrease. The maximal acid capacity of these materials can reach 0.7 mmol H^+/g and their proton
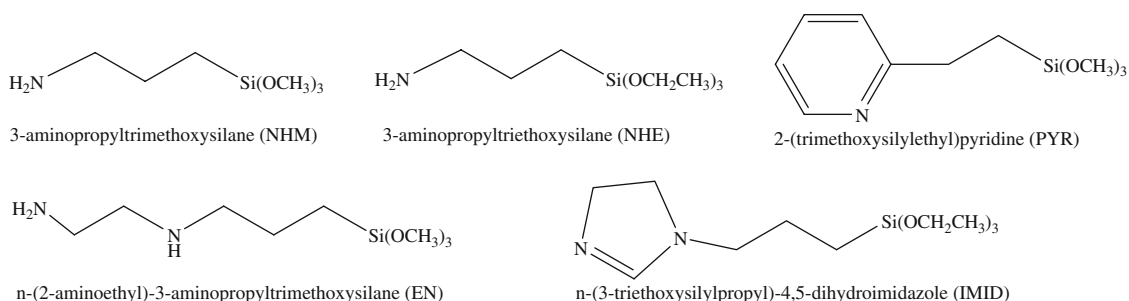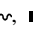
Scheme 6 Amino-containing trialkoxyorganosilanes
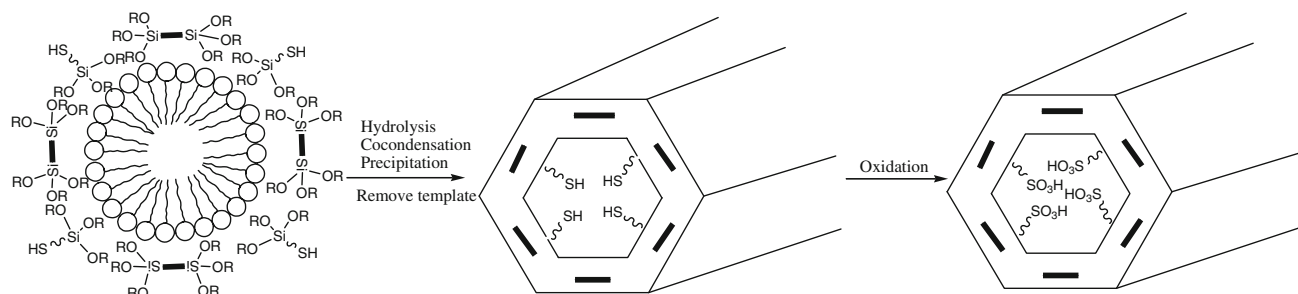
Scheme 7 Schematic representation of the synthesis of organo-functionalized PMOs by using both bridged organosiloxane precursors and terminal organosiloxane precursors in the presence of surfactant. (Surfactant, bridged organosiloxane precursors and terminal organosiloxane precursors are represented as O∿∿, ▬, ◄, respectively)

conductivity are appreciable. Yang and coworkers [97] synthesized thiol-functionalized PMOs by a similar method except to change the oxidant from aqueous H_2O_2 to concentrated HNO_3. Then PMOs are obtained with a maximum of incorporation of 3.45 mmol g^{-1} MPTMS into the mesoporous network. The thiol-functionalized PMOs oxidized by concentrated HNO_3 have higher acid exchange capacity with a maximum value equal to 1.38 H^+ mmol g^{-1}. These materials have a good thermal stability which is attributed to the higher stability of the benzene-bridged framework. Hamoudi et al. took advantage of both the organic surface functionalization via cocondensation procedure and the benefits of bridged mesoporous organosilica to synthesize arene-sulfonic acid functionalized ethane–PMOs [98]. By comparison, propyl-sulfonic acid functionalized ethane–PMOs are also synthesized and the acid capacity was assessed by acid–base titration. The oxidation process using hydrogen peroxide incompletely converted the thiol groups to sulfonic acid moieties. But the conversion of arene-sulfonic acid functionalized ethane–PMOs is much higher than the propyl-sulfonic acid functionalized PMOs. Furthermore, the acid capacity and proton conductivity of the arene-sulfonic acid bearing materials is higher than that of the propyl-sulfonic acid counterparts.

This kind of PMOs has also been synthesized by incorporating bridge bonded ethylene groups into the wall and terminally bonded vinyl groups protruding into the channel space. The bridging ethylene plays a structural and mechanical role while the vinyl groups are readily accessible for chemical transformation. The chemical and physical properties of the resulting bifunctional PMOs could be further modified [99]. The vinyl groups in the material undergo hydroboration with $BH_3 \cdot THF$ and the resulting organoborane in the bifunctional PMOs is quantitatively transformed into an alcohol using either $H_2O_2/$ NaOH or $NaBO_3 \cdot 4H_2O$. After subsequent in situ reactions the materials retain ordered structure. The vinyl-to-ethanol conversion in the vinyl/ethylene PMOs proceeds with surprising selectivity despite the chemical similarity between the terminal vinyl groups and the bridging ethylene groups in the framework. Functional organic groups in the framework are accessible for further reaction, but appear less reactive than terminal groups. The difference in reactivity could be attributed to steric factors, electronic difference associated with the π electrons and polarity of ethylene and vinyl groups.

2.2.2 PMOs with two kinds of bridged organic groups

There are only a few reports on the synthesis of bifunctional PMOs with two types bridging groups (Table 1, Class IV multifunctional hybrid materials) (Scheme 8). Markowitz and co-workers [100] attempted the synthesis of ordered bifunctional PMOs containing ethylene- and

Scheme 8 PMOs synthesized by two kinds of bridged organosiloxane precursors
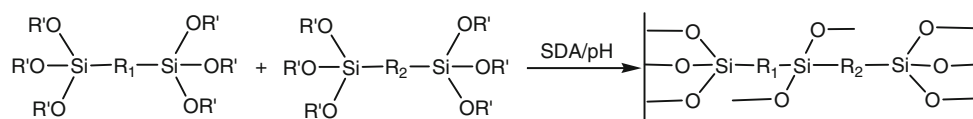
phenylene from rigid phenylene and ethylene- bridged precursors. The combination of functional phenylene/ethylene groups result in PMOs with a higher adsorption capacity than those only with one kind of organic group. The cross-polarization (CP) kinetics of the inner-chain carbons shows some difference between the composites with different organic bridges [101].

The synthesis of bifunctional PMOs containing $-CH_2-CH_2-$ and $-CH=CH-$ bridges in the wall was also reported. The distribution of organic groups in PMOs can be controlled using prehydrolysis of organosilica precursors [102]. In joint prehydrolysis condition the distribution of the two organic groups is homogeneous. However, when separate prehydrolysis condition was used, PMOs consisting of segregated regions of $-CH_2CH_2-$ and $-CH=CH-$ bridges within the same mesostructural framework were obtained. Analysis of the CP kinetics of these bifunctional materials indicates that the template–framework interaction is affected by the nature of the incorporated functional bridges. The $-CH_2CH_2-$ is more mobile in comparison with the $-CH=CH-$. The reason is assigned to their different locations in the framework. The ethene- bridges with reduced mobility are located in the bulk of the pore wall while the ethane-bridges are placed at the hybrid wall interface [103]. In addition, the mobility of surfactant head groups is reduced in composites with $-CH=CH-$ bridges, which could be attributed to the effect of increased electron density on the surface due to presence of sp^2 carbons.

Earlier, attempts to synthesize PMOs with large bridged groups, such as isocyanurate (ICS) groups, have yielded materials with either a small percentage of the bridged groups or poorly ordered mesostructures. Recently, isocyanurate-containing silsesquioxane-bridged bifunctional ICS-Et-PMOs have been successfully synthesized by co-condensation of tris[3-(trimethoxysilyl)propyl]isocyanurate and BTESE with a wide range of component variation of ICS-Si and Et-Si [104]. The core of tris[3-(trimethoxysilyl)propyl]isocyanurate is an isocyanurate ring integrated with three silicon atoms through flexible propyl chains. In the case of ICS-Si, its inductive effect on Si atom is similar to that of the moiety Si–CH_2CH_2–Si, which is favorable to the formation of well-ordered mesostructures. Moreover, the polarization effect plays a critical role in the fast hydrolysis and polymerization of the ICS-Si and subsequent formation of well-ordered bifunctional Et-ICS-PMOs. However, with increasing concentration of ICS bridging groups, their BET surface area, pore volume, and pore size decrease together with gradual deterioration of

mesoporous structure [105]. This is reasonable considering the geometrical constriction to accommodate a large number of bulky ICS bridging groups in the wall.

Because of comparable chemical reactivity which reduces the problems of phase separation during the syntheses, as well as the small size of the organic spacer groups of the organosilica precursors [2,5-bis(triethoxysilyl)thiophene and BTEB], the contents of thiophene and benzene bridging groups in bifunctional PMOs can be varied over a wide range without any decrease of mesostructural order and porosity properties [106]. Therefore, it is possible to tailor the surface properties of these PMOs which possess a combination of aromatic benzene and heterocyclic thiophene functional groups incorporated into the pore wall. When the amount of thiophene units were increased, the surface area of the products decreased, whereas the pore diameters increased. On the other hand, the framework wall thicknesses increased with decreasing content of thiophene groups in the framework.

The aniline trimer-contained hybrid siliceous materials were used to covalently distribute other aniline oligomers or amine-capped compounds into silica frameworks [107, 108]. For example, Garcia et al. recently reported the synthesis of photoresponsive porous silica by using the silicon precursor of *trans*-1,2-bis[*N*-(trimethoxysilylpropyl)pyridiumyl]-ethylene (*t*-BES) [109]. The strong electron acceptor viologen moieties were chemically grafted into the silica framework. Zhu et al. [110] reported the synthesis of bridged amine-functionalized PMOs by co-condensation of BTESE and N,N′-bis[3-(trimethoxysilyl)propyl] ethylenediamine (BTSPED) with block copolymer P123 as the template. Pore diameters which were mainly in the range 4–8 nm were observed to depend on the concentration of triblock copolymer used in the synthesis. Many of the bistrialkoxyorganosilanes containing amines or sulfides (e.g., bis[3-(trimethoxysilyl) propyl]ethylenediamine, bis[3-(triethoxysilyl)propyl] tetrasulfide) have flexible organic spacers. However, polymers formed from these precursors lack the structural rigidity to form ordered mesoporous structures. Removal of surfactants from the ordered mesoscopic composites of these monomers results in matrix collapse. Therefore, these resulting materials are disordered and exhibit relatively low surface areas.

2.2.3 PMOs with several kinds of bridged organic groups

PMOs containing more than two functional groups in the framework with ordered porosity are synthesized by using

three kinds of bridged organosiloxane precursors. For instance, benzene (BENZ), diethylbenzene (DEB), and ethylenediamine (EDA)-bridged bistrialkoxy precursors are used in the synthesis of multifunctional PMOs [111]. The PMOs containing both aromatic and metal chelating bridging groups are capable of removing aromatic organic pollutants as well as metal ions with high adsorption capacity while maintaining an ordered pore structure. The nature of the aromatic group is an important factor in the adsorption efficiency of the resulting PMOs. Replacement of a relatively small fraction of benzene groups with diethylbenzene resulted in much better sorption ability for *p*-chlorophenol. In addition to the efficient removal of phenol and copper ions, such PMOs copolymers can also be easily regenerated. Cho et al. [112, 113] reported the synthesis of spherical bifunctional and trifunctional PMOs particles, containing a combination of phenylene, thiophene, and ethane bridging groups. The structure ordering, surface properties, and morphology of this material can be tailored using different molar ratios of the organosilica precursors of 1,2-bis-(triethoxysilyl)ethane (BTESE), 1,4-bis(triethoxysilyl)benzene(BTEB), and 2,5-bis(triethoxysilyl)thiophene (BTET). In particular, the bifunctional phenylene-ethane PMOs and trifunctional PMOs exhibited spherical morphology with only a small amount of linkage among the particles. Also, the multifunctional PMOs spherical particles with 2D hexagonal mesostructure exhibited large specific surface areas and large pore diameters with uniform pore size distributions.

3 Influence of synthetic parameters

The formation, morphologies and structure of PMOs depend dominantly on the synthesis condition [114]. Many factors should be considered to obtain specific PMOs. Included are precursors, especially the related kinetics of their hydrolysis and condensation; template (cat-, an-, or non-ionic); the concentration of template (micellar or liquid crystal); inorganic species; pH (acidic or alkaline), temperature (low temperature or hydrothermal) and synthesis reaction time; additives (inorganic salts and organic molecules); order of mixing; solvent (aqueous or non-aqueous) and solvent composition; synthesis methods(evaporation induced self-assembly or precipitation). Furthermore, if physical shape of product need be formed (monolith, film, fiber or powder), the synthesis condition should be adjusted much finely [115].

3.1 Structure directing agent

As structure directing agents or templates, various surfactants, including cationic, non-ionic, divalent and binary surfactant, have been employed (Table 3). The interaction of ionic surfactants, either under acidic conditions ($S^+ X^- I^+$) or basic conditions ($S^+ I^-$) [116], is achieved by Coulombic force which is relative to the charge of surfactant(S) as well as inorganic species(I), and negative ion(X) in the inorganic salts(S^+ is the cationic surfactant, X^- is the counter ion provided by inorganic salt, and I^+ is a protonated Si–OH moiety and the overall charge balance is provided by association with an additional counter ion). Moreover, the formation process of mesoporous materials may involve a colloidal phase separation mechanism (CPSM) which is also believed to be related to the specific interaction of surfactant head groups and inorganic species in solution [117].

In acidic media, mesostructures have been obtained by using nonionic ethylene oxide surfactants and poly(alkylene oxide) block copolymers in acid media via an $(S^0H^+)(X^-I^+)$ synthesis route [118]. In contrast, the precursors of mesoporous materials are weakly interacting with the head groups of the surfactants (viz. by H-bonding) through S^0I^0 and N^0I^0 assembly interaction under neutral

Table 3 Currently available library of surfactants used to synthesize PMOs

Template		Interaction	Examples of surfactant
Ionic surfactant	Alkyltrimethylammonim halides (ATMA)	Charge-matching $I^- S^+$ or $S^+X^-I^+$	C_{16}TABr/Cl and C_{18}TABr/Cl [121]
	Divalent surfactant		$[C_nH_{2n+1}N(CH_3)_2(CH_2)_3N(CH_3)_3]^{2+}2Br^{2-}$ ($n = 16$, 18), shortened form: C_{16-3-1}, C_{18-3-1} [125]
Nonionic surfactant	Brij oligomeri	S^0I^0 and N^0I^0 or $S^0H^+X^-I^0$	Polyoxyethylene(10) stearyl ether (Brij 76) [131]
	Block copolymer		Triblock colymer F127 ($EO_{106}PO_{70}EO_{106}$) [138]
Binary surfactant	ATMA+ divalent surfactant	Multiple interaction depend on the diversity of used surfactant	C_{18}TABr and C_{18-3-1} [144]
	ATMA+Bri oligomeric		$(C_{18}$TMACl) and $C_{12}(EO)_4$; Brij-30 [145]
	ATMA+CF_4		C_{16}TABr and FC_4 [148]
Both hard and soft template	Surfactant and surface with regular patterns	Mechanical forces and S–I interaction	C_{16}TMACl and glass substrates with photolithographic lift-off [151]

condition (N^0 represents a nonionic surfactant) [5]. The progressively increasing surfactant concentration drives the organization of the surfactant into lyotropic liquid crystalline mesophases. The inorganic species in solution can be aggregated by specific assembly interaction. The formed material will have a corresponding structure from lyotropic liquid crystalline mesophases. Among those are commonly 2D or 3D hexagonal, cubic, and lamellar as well as variation of these structure [119].

3.1.1 Cationic surfactant

The surface-active molecules commonly used for PMOs synthesis are cationic alkyltrimethylammonium halides (ATMA) with various length of alkyl chain. A series of alkyltrimethylammonium bromide (C_nTAB) surfactants with different alkyl chain length ($n = 12, 14, 16, 18$) have been used as supramolecular template for synthesis of ethylene-containing PMOs [120]. Among all of the cationic surfactants, ATMA with alkyl chains having 16 and 18 carbon atoms has commonly been used for the preparation of PMOs [121]. Depending on concentration and condition, ATMA can forms hexagonal (2d, $p6$ mm), cubic (Ia-3d) and lamellar mesophases in a ATMA–water binary system and also in a inorganic–ATMA–water ternary system [45]. The synthesis system of BTME–ATMA–H_2O is typical because the system has formed a variety of highly ordered mesoporous materials with well-defined external morphologies [28].

The surfactant alkyl chain length proved to be a key parameter greatly influencing both the morphology and the porosity of the synthesized materials [122]. In the case of ethylene-containing PMOs, for example, the PMOs exhibit molecular-scale ordering within the organosilica framework and tunable pore size, depending on the alkyl chain length of the surfactant templates. Furthermore, depending on the alkyl chain length of the templates, the particle morphology of the ethene-PMOs gradually changes from monodisperse spheres (for $C_{12}TAB$) to rod or cake-like particles (for $C_{14}TAB$) and elongated ropelike particles for longer chain surfactants. For surfactant chain length up to 16 carbon atoms, spherical or truncated rhombic dodecahedral particles of different sizes were obtained for ethylene-PMOs. In contrast, in the presence of $C_{18}TMACl$ surfactant, the synthesized ethylene-PMOs exhibited particles almost entirely comprised of facetted rods.

ATMA with different halide atoms and their mixed system also influence PMOs synthesis. The rationale is based on their different solubility and phase behavior. Under the same experimental condition, while keeping the total surfactant concentration unchanged, a gradual increase of cetyltrimethylammonium bromide ($C_{16}TABr$) concentration vs. $C_{16}TMACl$ concentration, for instance,

could lead to systematic change of the crystallization behavior [123]. When gradually mix $C_{16}TABr$ into the $C_{16}TMACl$ system, the morphology changes continuously from highly branched large 4-fold "snowflakes" to crystals with few side branches, and even "holy crosses" with no side branches. At an even higher $C_{16}TABr$ concentration, regular small crystals, rather than dendrites, are formed. The addition of $C_{16}TABr$ caused the morphology to change from dendritic structures to more compact structures. It is speculated that $C_{16}TABr$ either changes the surface chemistry of the crystals, or the concentration of soluble species that are available to grow the crystals.

The use of divalent surfactants as SDAs to create PMOs is rare. Divalent surfactant molecules of C_{n-3-1} [$C_nH_{2n+1}-N(CH_3)_2(CH_2)_3N(CH_3)_3$]$^{2+}2Br^-$ are found unique to direct the formation of PMOs with different symmetry. The control of using C_{16-3-1} as an SDA for cubic Fm3m mesophase was corroborated by utilizing surfactants C_{16-3-1}, [$CH_3(CH_2)_{17}N(CH_3)_2(CH_2)_3N(CH_3)_3$]$^{2+}2Br^-$($C_{18-3-1}$), and [$CH_3(CH_2)_{15}N(CH_3)_3$]$^+Br^-$($C_{16}TABr$) as SDA [124]. Surfactants C_{18-3-1} are found to encode for PMOs of both [SBA-1]-n and [MCM-41]-n with cubic Pm3n while C_{16-3-1}, and $C_{16}TABr$ are found to encode them with hexagonal P6mm symmetry. Liang and coworkers used divalent surfactant [$CH_3(CH_2)_{15}N(CH_3)_2(CH_2)_3N(CH_3)_3$]$^{2+} 2Br^-$ (C_{16-3-1}) as SDA and BTESE as precursor to prepare highly ordered PMOs under basic condition [125]. The results showed that lower divalent surfactant concentrations C_{16-3-1} caused a mesophase transformation from cubic Fm3m to hexagonal P6mm symmetry.

3.1.2 Non-ionic surfactant

A variety of non-ionic surfactants such as alkylpoly (ethylene oxide) oligomers, namely Brij 56 [$C_{16}H_{33}(OCH_2CH_2)_{10}$–OH, [126, 127] denoted $C_{16}EO_{10}$] and Brij 76 ($C_{18}EO_{10}$) [128, 129] or triblock copolymer (PEO$_x$PPO$_y$/PBO$_y$PEO$_z$), also have been used, where PEO, PPO and PBO stand for poly (ethylene oxide), poly (propylene oxide) and poly (butylene oxide), respectively.

For longer chain bridged organic groups or larger oligomeric building units, it is necessary to employ a template of sufficient diameter to allow uniform encapsulation by polymerizing bridge-bonded silsesquioxanes. The nonionic alkylethylene oxide surfactant Brij 56 oligomeric surfactant proved to be suitable [130]. Burleigh et al. [131] synthesized PMOs with high surface area, ordered pore channels and pore size as large as 5.0 nm by using Brij 76 under acidic condition that do not break the hydrolytically labile sp^2 carbon to silicon bonds. Also, Brij 76 has better template stability during synthesis owing to the relatively lower solubility in ethanol. Additionally, compared with cationic surfactant, the supramolecular assemblies of nonionic Brij

76 in water may be constituted primarily of the hydrophobic carbon alkyl chains in the core and the many oxyethylene groups on the surface. Thus PMOs precursors containing nonpolar organic bridging groups had better interaction with nonionic Brij 76 than the highly charged surfaces produced by the C_nTABr surfactant.

Most of PMOs synthesized by using cationic alkylammonium surfactants and neutral amines afford pore diameters below about 5 nm [128, 132]. Block copolymer templates can yield larger structural features. Typical examples are triblock $PEO_x–PPO_y–PEO_x$ copolymers which have been widely used for preparing mesoporous silicas such as SBA-15 and SBA-16 [133]. The synthetic route of employing such nonionic block copolymers has such advantages as forming thicker wall, nontoxicity, and easy removal of the template. For instance, Muth et al. [134] prepared PMOs using the commercially available triblock copolymer P123 ($PEO_{20}PPO_{70}PEO_{20}$) as the surfactant together with BTME as the organically bridged silica source. The PMOs obtained have pore diameters as large as 6.5 nm, a wall thickness of at least 5.9 nm and BET surface areas greater than 900 $m^2 g^{-1}$.

The pore sizes of PMOs are also dependent on the hydrophobicity and critical micelle concentration (CMC) value of block copolymer templates [135, 136]. Moreover, the critical micelle concentration (CMC) value of block copolymers could be a powerful criterion for the experimental design of the synthesis of ordered mesoporous materials [137]. Block copolymer surfactants that have small CMC values will template ordered silica mesoporous materials with certain structures (hexagonal, cubic, vesicle, etc.); on the contrary, surfactants that have large CMC values will give rise to disordered mesostructures. Cho et al. [138] synthesized mesoporous organosilicas by the co-condensation of TEOS and BTME by using triblock copolymer templates such as F127 ($PEO_{106}PPO_{70}PEO_{106}$) and poly-(ethylene oxide)-poly(DL-lactic acid-co-glycolic acid)-poly(ethylene oxide) (PEO-PLGA-PEO). When F127 triblock copolymers are employed as SDA, pore size is as large as $d_{p, max} = 58.5$ nm for PMOs. Compared with the PPO blocks in the PEO–PPO–PEO block template, PLGA blocks in the PEO–PLGA–PEO block templates are more hydrophobic. As to PEO–PPO–PEO, a small difference of hydrophilicity between PEO block and PPO block is not so effective for forming PMOs with a large amount of BTME incorporated. But with regard to incorporation of organosilica into the framework of PMOs, the more hydrophobic PEO–PLGA–PEO triblock copolymer is more effective than the PEO–PPO–PEO triblock copolymer template. Therefore, it is possible to adjust the pore size of mesoporous materials by changing their structural parameters of block copolymer surfactants [113, 137].
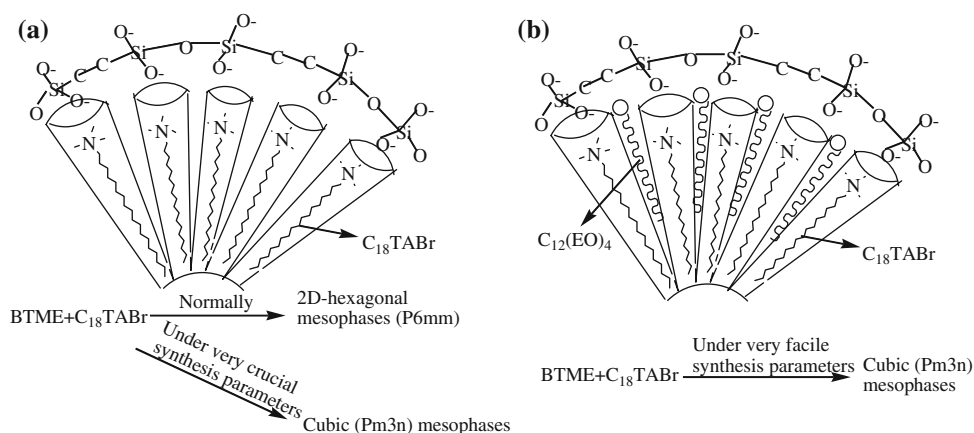
The more hydrophobic poly(butylenes oxide)-containing triblock copolymer $PEO_x–PBO_y–PEO_x$ also have been used to synthesize PMOs with large pores [139]. Matos et al. [140] synthesized PMOs with very large cage-like pores by using triblock copolymer template ($PEO_{39}PBO_{47}PEO_{39}$, B50-6600) and Pluronic P123, respectively. The pore diameter of PMOs synthesized using triblock copolymer P123 with PPO block is much lower than that of SBA-15 silica synthesized using the same template under similar condition, whereas the pore diameter of PMOs synthesized using the B50-6600 template with block is similar to that of FDU-1 silicas. This suggests that the organosilica structure has a higher tendency than the silicate structure to occlude hydrophobic polymer chains, and thus the template with a more strongly hydrophobic block, such as the PBO block, appears advantageous in the synthesis of large-pore PMOs [138]. At room temperature, there are small differences of hydrophilicity/hydrophobicity among PEO, PPO and PBO chains and the hydrophobicity of these blocks follows the sequence of PBO > PPO > PEO [141].

3.1.3 Binary surfactant mixtures

From the point of view of colloid chemistry, mixed-surfactant systems have the different packing parameters of aggregated surfactants. Therefore, the system of mixing surfactants appears different from that of the corresponding system of single surfactant [142]. Hence, such knowledge can be considered for the synthesis of PMOs with tunable pore sizes and structures [143]. A series of ordered PMOs with cubic (*Pm3n*) and hexagonal (*P6mm*) symmetry have been synthesized from organosilica precursor BTESE by using cationic surfactants $C_{18}TABr$ or $[CH_3(CH_2)_{17}NMe_2 (CH_2)_3NMe_3]^{2+} 2Br^- C_{18-3-1}$ or binary mixtures (C_{18-3-1} and $C_{18}TABr$) as structure directing agents [92, 144]. The formation of hexagonal PMOs and cubic PMOs can be efficiently controlled by the concentration of the single component surfactant as well as by the concentration and ratio of the corresponding binary surfactant mixtures. The mesopore range (2.9–4.0) is adjusted via the ratio and amount of binary surfactant, where relatively low concentrations of binary surfactant mixture favored the formation of smaller pores with longer range structural ordering.

Binary surfactant mixtures composed of polyoxyethylene alkyl ether [$C_{12}(EO)_4$; Brij30] and octadecyltrimethylammonium chloride ($C_{18}TMACl$) have been used to synthesize cubic hybrid ethane-silica mesoporous structures with well-defined dodecahedral morphology [145]. The order and morphology strongly depended on the hydrolysis and condensation kinetics of BTME in the presence of different ratios of mixed surfactants. In the BTME–ATMA–NaOH–H_2O system, the typical geometry of ethane-bridged

(a)

C$_{18}$TABr

BTME+C$_{18}$TABr $\xrightarrow{\text{Normally}}$ 2D-hexagonal mesophases (P6mm)

$\xrightarrow{\text{Under very crucial synthesis parameters}}$ Cubic (Pm3n) mesophases

(b)

C$_{12}$(EO)$_4$ C$_{18}$TABr

BTME+C$_{18}$TABr $\xrightarrow[\text{synthesis parameters}]{\text{Under very facile}}$ Cubic (Pm3n) mesophases

organosilica molecules resulted in the formation of two-dimensional hexagonal mesophases (*P6mm*). Under very crucial synthesis parameters, the cubic (*Pm3n*) mesophases can be obtained [45]. With addition of C$_{12}$(EO)$_4$ surfactant into BTME–C$_{18}$TMACl system, cubic (*Pm3n*) mesophases can be formed because the low surface concentration and subsequent polymerization may well lead to the contraction of the micellar surface, resulting in phase transition from two-dimensional hexagonal (*P6mm*) to cubic (*Pm3n*). It is possible that the C$_{12}$(EO)$_4$ surfactant penetrates into the hydrophobic and palisade regions of the surfactant arrays and thereby induces a structural rearrangement of the surfactant phase to re-optimize the interface charge density matching and surfactant packing (Scheme 9).

Fluorocarbon surfactants [C$_3$F$_7$O(CFCF$_3$CF$_2$O)$_2$CFCF$_3$-CONH (CH$_2$)$_3$N$^+$(C$_2$H$_5$)$_2$CH$_3$I$^-$, (FC$_4$)] are a kind of stable surfactant used at higher temperature (>200 °C). Due to the rigidity and strong hydrophobicity of the fluorocarbon chains, fluorocarbon surfactants cannot form an ordered surfactant micelle quickly, and therefore these fluorocarbon surfactants are not well suitable as template for the preparation of well-ordered mesoporous materials [146]. However, when a fluorocarbon surfactant is mixed with another surfactant to form a mixture, it becomes more suitable as the template [147]. For instance, once a binary surfactant system of fluorocarbon surfactant FC$_4$/cationic surfactant C$_{16}$TABr was employed as costructure directing agents and BTME as the hybrid silica precursor, a novel hollow-spheric PMOs with tunable wall thickness was obtained. The mechanism is postulated to be a new vesicle and a liquid crystal "dual templating" procedure [148] (Scheme 10).

3.1.4 The hard template

To obtain porous organosilicas with both macroscopic and microscopic ordering, the so-called hard template method through microchannels, patterns, and surface interactions
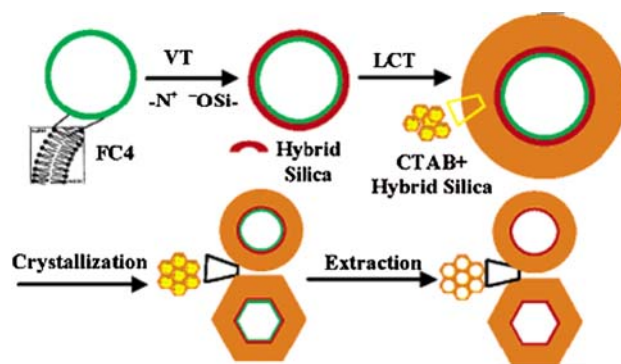
Scheme 10 Schematic representation of the vesicle templating (VT) and the liquid crystal templating (LCT) dual templating process. Adapted from [148]. Copyright 2006, with permission from American Chemical Society

was developed [149] (Scheme 11a). The 2D hexagonal structure is made of close-packed, long rod-like micelles. In most cases, these rod-like micelles are aligned along lithographically defined pore channels and the longitudinal directions of micropatterns on surface [150]. However, self-assembled structure such as cubic phases is made of close packed spherical micelles or bicontinuous micellar structure. One may be able to rely on the anisotropic physical confinement or mechanical forces to align the packed spherical micelles that are associated with the cubic phases.

Hybrid organic silane BTME along with surfactant C$_{16}$TMACl have been used to grow large ordered arrays of PMOs crystals on patterned substrates [151]. Patterns of gold triangles and lines were created on glass substrates using a photolithographic lift-off technique. The gold micropatterns were made hydrophobic by immersing the substrate in an ethanol solution containing alkane thiol molecules, which favors the growth of mesophase materials. The ethane-PMOs grown on the triangular patterns remain typical *Pm3n* cubic mesostructure and contain uniformly distributed organic groups (–CH$_2$CH$_2$–) within
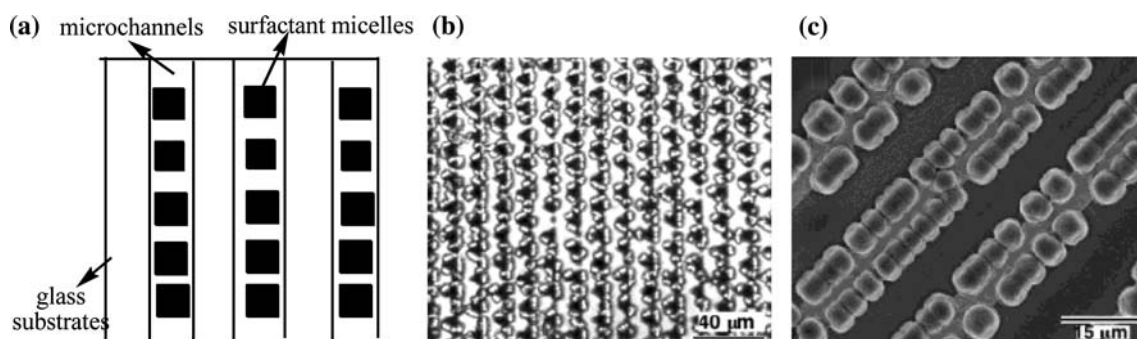
Scheme 11 Alignment of self-assembled crystals on patterned substrates. **a** Schematic representation of the growth of oriented nanoporous materials. **b** Patterned and aligned crystals on triangular micropatterns. **c** Patterned crystals on lines and the right panel shows the morphologies of crystals on line patterns. Adapted from [151]. Copyright 2003, with permission from American Chemical Society

the framework. The nucleation and growth of mesophase crystals in general followed the triangular micropatterns. The liquid crystal ordering of surfactant micelles during the synthesis remains important to the local order of the mesostructure (Scheme 11b). In addition, the geometry of the underlying patterns has an effect on the crystal morphology of the self-assembled crystals. Unlike the crystals on the triangular patterns, those on the line patterns mostly do not have a well-defined shape (Scheme 11c) and therefore no clear preferred crystalline orientation alignment. These findings could be used to control the crystal orientation and morphology by optimizing and matching the geometry of the micropatterns with that of the crystals to be grown.

3.2 Inorganic salts

Inorganic salts have an influence as observed from the block polymer-assisted synthesis of PMOs [152, 153]. These results can be attributed to the specific effect of inorganic salts on the self-assembly interaction between surfactant head groups and inorganic species. For block copolymer surfactants with large critical micelle concentration value, the use of inorganic salts causes dehydration of ethylene oxide units from the hydrated PEO shell adjacent to the PPO core, leading to an increase in the hydrophobicity of the PPO moieties and a reduction in the hydrophilicity of the PEO moieties [154]. By the counter ion mediated $(S°H^+)(X^-I^+)$ pathway, the low hydrophilic PEO head groups in the positively charged surfactant are expected to have increased interaction with the positively charged organosilane species with low hydrophilicity because of the organic components. This enhanced self-assembly interaction can result in a long range ordered domain of organosilica surfactant mesostructure.

Various alkali metal salts such as sodium halide (NaF/Cl/Br/I), potassium halide (KF/Cl/Br/I) and alkali sulfates (Na$_2$/K$_2$SO$_4$) have been employed to improve hydrothermal

stability during the crystallization process [155–157]. Contrary to previous conclusions that highly ordered PMOs can only be synthesized in a limited range of low acid concentrations, high quality large-pore PMOs can be prepared over a wide range of acid concentrations by the addition of inorganic salt [158]. The presence of KCl is believed to weaken the disturbance of the organic moiety and enhance the interaction between the template and the organosilica [159]. Namely, the salts may favor the interaction between non-ionic block copolymer head groups and the oligomers produced by the hydrolysis and condensation of organosilica precursors [160]. However, exclusively rod-like morphology can only be obtained in a narrow range of acid and salt concentration. Such alkali sulfates as Na$_2$SO$_4$ and K$_2$SO$_4$ have been used as auxiliary agents in the synthesis of large-pore hexagonal PMOs with long-range structural order [161]. For the same reactant components but without inorganic salts, only amorphous gel was obtained. The well-ordered PMOs with Im3m symmetry could be prepared in the presence of Na$_2$SO$_4$ instead of K$_2$SO$_4$. The use of NaCl or KCl resulted in the deterioration of the long-range order of PMOs [162].

In addition, the formation of mesoporous solids is relative to the kind of Hofmeister anions in their corresponding inorganic salt [163–165]. The highly charged salts usually favor the formation of the single crystals [162]. During the synthesis of ethane-silica and benzene-silica PMOs in the presence of poly(ethylene oxide)-containing nonionic triblock copolymers, the addition of KCl, CaCl$_2$, and AlCl$_3$ causes an increase in the BET surface area and the pore volume, and a decrease in the pore diameter and the wall thickness [166]. For yield highly ordered 2D hexagonal benzene-PMOs, a small amount of AlCl$_3$ can serve as a new promoter mediating supramolecular interactions between PEO chains and BTEB precursor. Moreover, it is possible that AlCl$_3$ has a comprehensive influence on the synthesis of PMOs by promoting the formation of polymeric micelles

and controlling pH of the synthesis gel because $AlCl_3$ is a strong Lewis acid.

3.3 Organic additives

The effect of organic additives as expander molecules or co-surfactants has been previously reported for mesoporous pure silicas [167, 168]. Namely, the pore size and pore volume of this material can be enlarged by adding organic swelling agent, for example, trimethylbenzene (TMB). However, a disordered foam-like phase gradually forms. Besides, organic additives have dramatic effects on the morphology of the obtained products [169]. In these aspects, there are rare data for PMOs [144].

The presence of such an organic swelling agent as TMB can indeed afford a series of PMOs with pore sizes from 6 to 20 nm [170]. It is interesting to note that an increase in the pore-expanding agent gave not only larger pore sizes but also changes in mesostructure. When no TMB is added, the resulting organosilicas exhibit a wormhole motif with a pore diameter of approximately 6 nm. Moderate addition of TMB gives expanded wormhole structures (d_P = 12) and large amounts of TMB produce PMOs with hexagonal arrays of spherical pores (d_P = 20 nm). In another case of PMOs with large cage-like pores [171], the pore size of the 3-D ordered PMOs can reportedly be tuned in the range of 5.6–8.0 nm through adding a certain amount of organic additive organic additive, which also leads to a structural change from highly ordered to foam-like [172], but the pores were still cage-like and well-defined with a narrow distribution, and the total pore volume was be significantly increased. Nakanishi et al. [173] have studied spontaneously-formed hierarchical macro-mesoporous ethane-silica monolith. The micelle-swelling agent, an organic additive TMB, that enhances the self-organization of structure directing agents and has been successfully used to give hierarchical well defined macropores and highly ordered mesopores. The addition of TMB significantly stabilized the cylindrical micelles of P123, leading to the emergence of long-range order in the mesoporous arrangement. Further addition of TMB induced additional structural transformation.

Organic compounds as cosolvents can also affect the formation and properties of PMOs. For example, addition of butanol in conjunction with P123 under acidic condition afforded ethene-PMOs with much narrower pore size distribution and enhanced ordering compared with the materials synthesized without adding cosolvent [174]. Moreover, adding cosolvent ethanol leads to small pores, while the pore sizes were much larger when a longer chain alcohol, e.g., hexadecanol, was added as a pendent side chain [63]. In addition, addition of butanol was found to give rise to a large pore cubic (Ia3hd) mesophase instead of the more familiar SBA-15 hexagonal structure [175].

3.4 pH value, temperature and others

The acidity or basicity is one of key factors that determines the specific interaction between surfactant and organosilica precursor and also affects the mesostructural regularity of PMOs. The form of interaction of reactants is different at different pH value. For ionic surfactants, the framework-forming precursors of PMOs are expected to be negatively charged and thus strongly bound by electrostatic interaction with the cationic head groups of the surfactant micelles (i.e., S^+I^- assembly) under basic condition [15]. As discussed above, PMOs can also be prepared by using cationic surfactant via the ''$S^+X^-I^+$'' route under acid conditions, by using nonionic surfactants via an ($S^0H^+X^-I^0$) route in acid media or by S^0I^0 and N^0I^0 assembly interaction under neutral condition [118, 176].

The mesostructural regularity of PMOs can be affected by the acidity of the solution [48]. Generally, slow condensation of organosilicate is desired so that continuous rearrangement and reinforcement of the organosilica network at the organic and inorganic interfaces occur and thus the structural formation is more thermodynamically favored. To slow their condensation rate of inorganic and organic, a convenient way is to use a relatively low concentration of acid. Burleigh et al. have synthesized mesoporous bifunctional organosilica materials by co-condensation of BTESE and N-(2-amino-ethyl)-3-aminopropyl-trimethoxysilane (AAPTS) under either acidic or basic condition [177]. However, if an ordered pore structure and faster access of molecular species to functional groups are required, then the base-catalyzed approach should be favorable. Nevertheless, under controlled low acid concentration, Bao et al. [48] have developed PMOs with highly ordered, large pores.

The influence of reaction temperature on PMOs products also exists. Zhou et al. found that the pore size of PMOs expands along with a decrease of temperature [178]. In addition, the level of silica condensation in the wall of mesoporous silica will be enhanced by increasing the crystallization temperature. As for micelle formation, the higher temperature is unfavorable (>150 °C). Therefore, PMOs are generally prepared at room temperature or relatively low temperature (80–150 °C). Aside from the change of pore, PMOs synthesized at different temperatures show a slightly different morphology [179].

The extent of agitation, from static condition to fast stirring condition, and the reaction time are also found influential on the structure and texture of PMOs [180]. For example, as to PMOs with hexagonal symmetry synthesized from octadecyltrimethylammonium bromide (C_{18}TABr) as template and BTME as organosilica source, with longer reaction time (21 h), the amount of worm-like shaped aggregates increases. With agitation, the rope-like morphology with low curvature disappears dramatically, while

most of products exhibit a variety of morphologies with a high curvature. A variety of hierarchical superstructure of PMOs that contain molecularly ordered ethylene groups are obtained by simply varying the extent of stirring (i.e., agitation of the synthesis gels) [181]. Under static condition, large (>10 mm in diameter) hierarchical cake-like particles made up of loosely or closely aggregated rods are obtained as the predominant particle morphology. Fast stirring condition generates spongy flower-like particles. Intermediate stirring condition results in a mixture of smaller cake-like particles and elongated rope-like particles that are made up of closely aggregated rods.

4 Applications

The rapid development of synthesis chemistry makes it feasible to introduce various desired functional groups into PMOs. As a consequence, such PMOs with multiple functionalities could find much more versatile applications than its pure inorganic counterparts. Among a variety of applications of PMOs, the greater potentials mainly lie in the fields of catalysis, environmental remediation, biology, analytical chemistry and microelectronics according to the reports in the literature.

4.1 The application in catalysis

Heterogeneous catalysis with high efficiency is an environmentally friendly route for the production of most of chemicals. Among those, the catalytic application of PMOs as heterogeneous catalysts is well-documented since the use of solid PMOs allows easier separation, recovery and recycling of the catalyst from the reaction mixture together with their multifunctionality of organic groups [182]. Moreover, besides its inorganic silica matrix and organic functionalities, incorporation of additional metal atoms in the framework is also viable for producing solid acid/base or redox catalysts. Therefore, combing organic groups and active sites of metal atoms in the hybrid frameworks with ordered porosity, a desirable catalyst could be put into practice [183].

4.1.1 Metal-containing catalysts

Introduction of heteroatoms into the frameworks as catalytically active sites in various mesoporous materials can expand the range of their applications in heterogeneously catalytic processes [184–187]. Before the discovery of PMOs, much research had been conducted on the loading of active metal species on porous inorganic silica-containing materials such as ZSM-12, ZSM-48, HMS [188, 189], zeolite β and MCM-41 [190], MCM-48 [191]. For

their highly hydrophobic surface properties, PMOs functionalized with metal species might offer significant advantages over the traditional silica-based materials due to the increased controllability of hydrophobicity/hydrophilicity of the surface of the pores as well as an enhanced functionality of the resulting mesoporous hybrids, which could yield some favorable catalytic performance [192].

Most of metal-containing PMOs are synthesized by using the terminal or bridged organic groups in organofunctionalized PMOs as a ligand to bind the metallic atoms [193]. Corma and co-workers [194] have synthesized PMOs with varying contents of carbapalladacycle complex. These materials exhibit catalytic activity for the Suzuki–Miyaura cross-coupling of bromobenzoic acid with phenylboronic acid (Scheme 12). The loading of carbapalladacycle complex has a remarkable influence on the catalytic activity. The highest turnover frequency (TOF) of 34979/h was observed for the PMOs with 0.008 mmol/g of Pd content. In addition, there exists the influence of catalyst structure on catalytic activity for Suzuki reactions.

The introduction of chiral ligands into PMOs is of special interest in chiral catalysis, because PMOs have a uniform distribution of organic moieties in the framework [195]. The nanopores of PMOs can be used as novel nanoreactors for heterogeneous asymmetric catalysis when the chiral catalysts are assembled in the nanopores of PMOs or incorporated in the framework of PMOs [196–198]. For example, the PMOs synthesized by cocondensation of some nitrogen-containing organosiloxane precursors have ability to anchor metal ions or organometallic groups for metal chiral catalysis (Scheme 13). Gigante et al. [79] synthesized a chiral vanadyl salen complex (VOsalen) (Scheme 13a) and used this chiral organosilane precursor in combination with TEOS to synthesize the corresponding VOsalen@ChiPMOs. The materials are chiral and showed enantioselectivity for the asymmetric catalytic cyanosilylation of benzaldehyde with TMSCN (Me₃SiCN). Yang et al. [108] synthesized mesoporous ethane-silicas with chiral ligands by the co-condensation of BTME and organosiloxane (Scheme 13b). These materials were used as catalysts for the asymmetric transfer hydrogenation of acetophenone after complexing Rh_2Cl_2
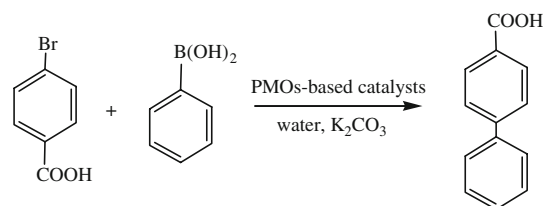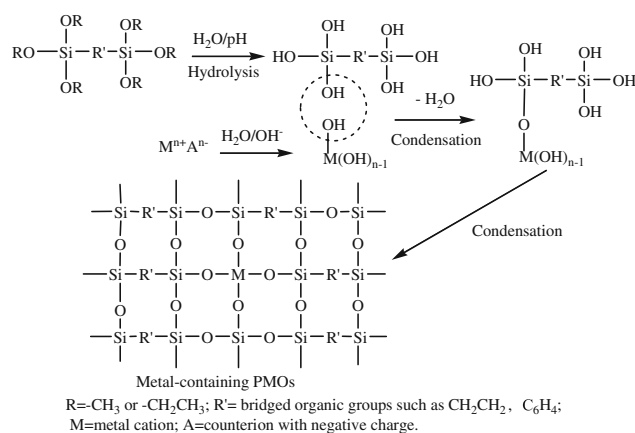
Scheme 12 The Suzuki–Miyaura cross-coupling of 4-bromobenzoic acid with phenylboronic acid in the presence of PMOs with a carbapalladacycle complex

$(C_8H_{12})_2$ (cyclooctadiene rhodium chloride dimer, [Rh(cod) Cl]$_2$) to the chiral ligands. It showed enhanced catalytic activity compared to the catalyst with pure-silica framework under identical reaction condition. Two types of trans-(1R, 2R)-diaminocyclohexane with benzyl/propyl groups (Scheme 13c, d) as a linker can be incorporated into the framework of PMOs [78, 199]. The catalyst [Rh(cod)Cl]$_2$ coordinated to the chiral diamino groups in the framework of PMOs with benzyl group as linker exhibits higher conversion and enantiomeric excess (ee = ([R] − [S]/[R] + [S] × 100%) value than its homogeneous counterparts for the asymmetric transfer hydrogenation of ketones. The comparison of the catalytic properties of the materials with benzyl and propyl groups as linkers indicates the importance of the rigidity and electron-withdrawing ability of the linker for the high catalytic reaction rate.

The above-mentioned procedures, however, are only appropriate for a small number of metal atom–organic functionality pairs [79]. Another strategy to synthesize the metal functionalized PMOs involves direct synthesis through the isomorphic substitution of the silicon atoms by such metal species of interest as Ti [200], Al [201], Ru [202], Cr [203], Zr [204], Pd [192], Mo [205], and V [206] in the synthesis of ethane-PMOs (Scheme 14). Almost all of these materials show a high hydrothermal stability and catalytic activity, which is attributed to the presence of hydrophobic ethane bridging groups. Titanium containing PMOs (Ti-PMOs) are well documented and have been found effective for the epoxidation of alkenes [184, 207–209] (Scheme 15a, b) and hydroxylation of phenols [210] (Scheme 15c) using aqueous H$_2$O$_2$ or tert-butyl hydrogen peroxide (TBHP)or O$_2$ as oxidants [209]. For example, Kapoor and coworkers [211] synthesized Ti-PMOs by

using BTME and TEOS as silica source and titanium butoxide (TBOT) as titanium source in presence of alkyl-trimethyl ammonium chloride. The catalytic activity was evaluated by the liquid phase epoxidation of α-pinene with hydrogen peroxide H$_2$O$_2$ selectively to α-pinene oxide (Scheme 15d). Compared to traditional titanium containing mesoporous silica (Ti-MCM41), the Ti-PMOs have improved catalytic performance due to the generation of active hydrophobic centers through an ethylene fragment that provides the possibility of incorporating more tetrahedrally coordinated titanium on the inner surface of the mesoporous silica. Also such catalysts display higher H$_2$O$_2$ efficiencies.

The preparation of metal-containing PMOs through the isomorphic substitution, however, also suffers from some

Metal-containing PMOs

R=-CH$_3$ or -CH$_2$CH$_3$; R'= bridged organic groups such as CH$_2$CH$_2$, C$_6$H$_4$; M=metal cation; A=counterion with negative charge.

Scheme 14 Schematic representation of the preparation of metal-containing PMOs catalyst through the isomorphic substitution of the silicon atoms by the metal species

Scheme 13 Nitrogen-containing organosiloxane used in the synthesis of the PMOs with chiral catalytic activity
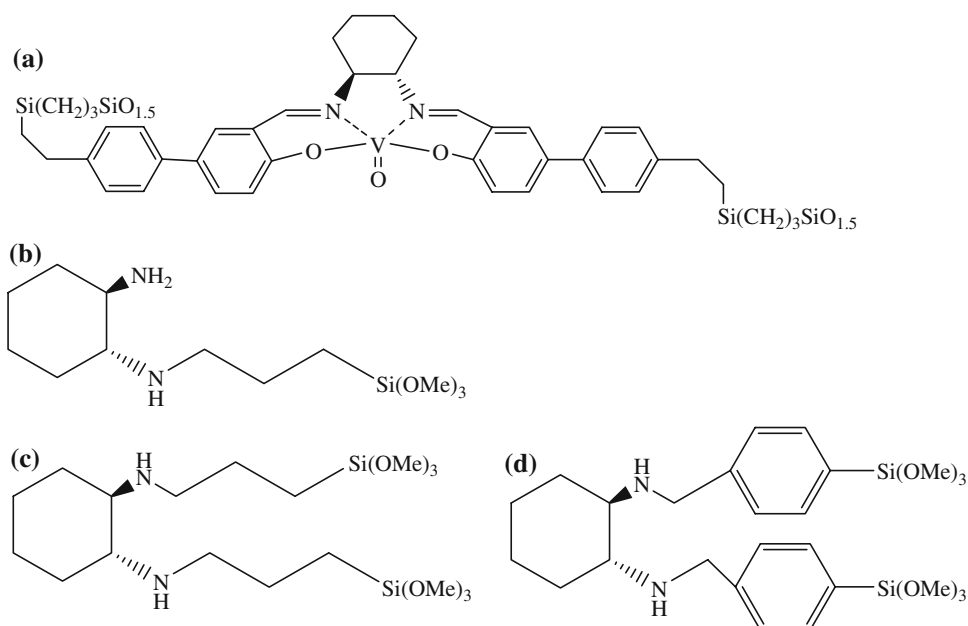
Scheme 15 The oxidation and expoxidation reaction catalyzed by Ti-PMOs
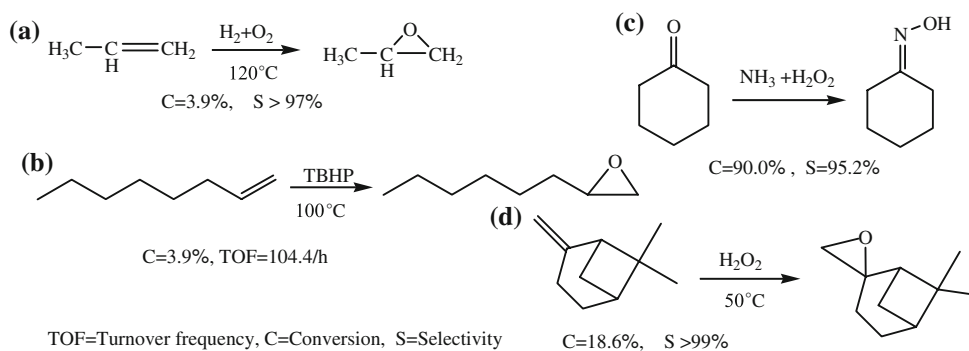
problems. It includes the difficulty for removing template, the loss of the ordered mesoporous structure and the morphological changes that occur with respect to loading. For the PMOs without incorporating metal species the removal of the template is usually achieved by acidic extraction from the ethanol media. It proves problematic for the Al-PMOs due to dealumination of the framework [212]. The modified template removal procedure can overcome this problem and thereby retain the tetrahedral coordination of aluminium during extraction process. Firstly, the template of as-synthesized Al-PMOs can be removed by heating the as-synthesized solid at 50 °C for 4 h with specially dilute HCl (8.8×10^{-3} M)/C_2H_5OH mixture [213]. Secondly, the removal of occluded surfactants without dealumination can be accomplished by substituting HCl/C_2H_5OH for EtOH–NH_4NO_3 mixtures [214]. The unit cell parameter and pore sizes of some metal-containing PMOs were enlarged slightly because of the incorporation of metal ions, which has ionic radii larger than that of silica, which leads to relatively longer metal–O bond distances [215]. Meanwhile, these metal-containing PMOs exhibited slit-shaped pore structures, which might indicate that some structural defects are formed in the channel matrix [216].

4.1.2 Solid acid/base catalysts

Increasing awareness of the environmental costs of traditional liquid acid/base-catalyzed processes has stimulated the development of solid acid/based catalysts. The discovery of PMOs has raised the general expectation that the catalytic efficiency can be improved by combining the properties of organic and inorganic components in such hybrid materials as well as their high surface area and larger pores. Additionally, since the framework of PMOs consists of homogeneous distribution of organic groups, they possess better hydrothermal stabilities than the conventional mesoporous silicas. For example, the Al-PMOs synthesized by one-pot condensation of BTME and aluminium isopropoxide (Al(O^iPr)$_3$) have improved catalytic performance in alkylation of 2,4-di-*tert*-butylphenol with
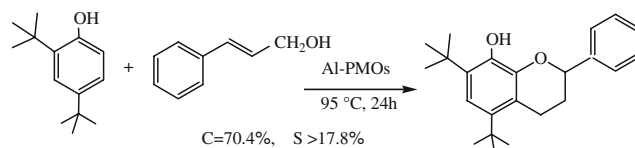
cinnamyl alcohol to yield a flavan (Scheme 16) due to their more hydrophobic character compared with Al-MCM-41 materials [217]. Aluminum-rich PMOs (Al-PMOs) have also potentials in such acid catalyzed organic transformations as acylation of aromatics, hydroisomerization and cracking reactions of bulky molecules.

When functionalized with sulfonic acid or arene sulfonic groups, PMOs can serve as acidic catalysts in reactions such as esterification, hydration, alkylation [218] and condensation [95]. Shylesh et al. revealed that the sulfonic acid functionalized organosilica materials synthesized were more active, selective and stable in the Claisen–Schmidt condensation of aldehydes and ketones (Scheme 17) than the conventional MCM-41 and an amorphous silica gel [93]. The high activity and stability of the sulfonic acid functionalized PMOs, possibly relates to the tight anchoring of the propyl –SO_3H groups in the inner pore walls as well as the hydrophobic environments imparted inside due to the presence of bridging organic groups.

However, in a sense the hydrophobicity of the framework does not always play an active role in the catalytic reaction. The presence of organic moieties in the mesoporous network, for instance, has a negligible contribution to the esterification reaction of acetic acid with ethanol and the sulfonic acid groups mainly contribute to the formation of ethyl acetate. Nevertheless, in its reverse hydrolysis reaction of cycloacetonate, both the hydrophobic nature and active catalytic sites are very important factors for enhanced product yields [97]. In addition, the catalytic activity of sulfonic acid-functionalized mesoporous organosilicas also differs with different bridging organic moieties in the


Scheme 16 Alkylation of 2,4-di-*tert*-butylphenol with cinnamyl alcohol in the presence of Al-PMOs

Scheme 17 Reactions of substituted benzaldehyde and acetophenone over PMOs-SO₃H catalyst
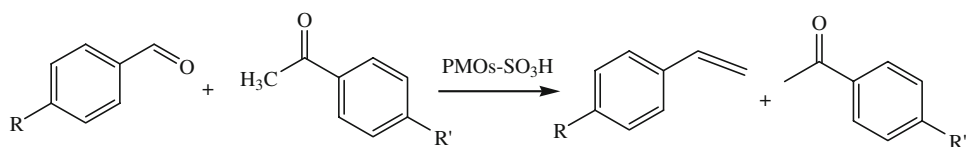
framework. The sulfonic acid-functionalized ethane- or benzene-bridged PMOs show high catalytic activity in the condensation of phenol with acetone to form bisphenol A [219]. But the activity of sulfonic acid-functionalized ethane-PMOs is higher than that of benzene-PMOs. One of the possible reasons is ascribed to the larger specific surface area and average pore diameter of the former.

Over the past decades, various organic and inorganic base catalysts, such as primary and tertiary amines and alkali metal hydroxides, carbonates, and alkoxides have been applied to the synthesis of fine chemicals and pharmaceuticals [220, 221]. Recently, amino- or diamino-modified porous silicas have proven to be effective heterogeneous base catalysts for a wide range of C–C forming reactions, e.g., Knoevenagel [222, 223], cyanosilylation [224], and Claisen–Schmidt condensation [225] (Scheme 18). Bifunctional PMOs with hydrophobic ethylene groups in the framework and hydrophilic reactive amine groups protruding into the pores are potential candidates as novel solid base catalysts. The nitrogen-containing functional groups can be amine, diamine, triamine groups, or cyclams originated from the direct one-step co-condensation of bridged trialkoxysilanes and amino-containing organosiloxanes. A typical example of such a material is "aminopropyl PMOs", prepared by functionalization of PMOs with (aminopropyl) trialkoxysilane in the presence of block copolymer Pluronic P123 under acidic conditions [159]. These materials display basicity typical of a simple amine. To evaluate the accessibility of the amine group in the amine- functionalized PMOs and their catalytic performance, nitroaldol condensation between nitromethane and benzaldehyde was tested as a model reaction. The results showed that the materials are highly active in the nitroaldol reaction of benzaldehyde and nitromethane (conversion > 99%, selectivity > 98%) and can be recycled.
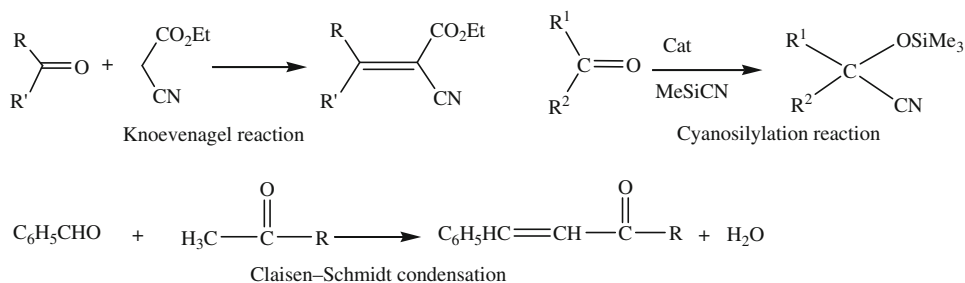
4.2 Application in pollution abatement

PMOs with uniformly bridged groups (such as ethane, benzene) usually are inert and hydrophobic, which is favorable for the physical adsorption of organic pollutants. Mark et al. have synthesized diethylbenzene- and ethylene-bridged PMOs by the hydrolysis and condensation of alkoxysilyl precursors under basic conditions and have investigated their adsorption of three phenolic compounds (4-nitrophenol, 4-chlorophenol, 4-methylphenol) by both batch and column testing [226]. All of these materials show high adsorption capacities, fast adsorption kinetics, and easy regeneration for the removal of phenols from wastewater. However, the arylene-bridged material adsorbed 14 times more 4-nitrophenol than the ethylene-bridged sorbent for the same surface area. The authors speculated that π–π interactions between the aromatic rings of the arylene-bridged sorbent and the phenolic compounds play an important role in the binding between them.

In addition, the functional groups in PMOs would be sufficiently reactive and hydrophilic to scavenge toxic anions and heavy metals from waste sources [227]. PMOs with functional groups such as isocyanurate (ICS) [71], mercaptopropyl, thiophene [66] and amino groups [87] are in particular promising in environmental cleanup for heavy metals from water [109]. For instance, chelating properties of the isocyanurate bridging group make the ICS-PMOs attractive adsorbents for heavy metal ions [63]. These ICS-PMOs have very high adsorption capacity toward mercury ions (1.8 g of Hg^{2+} per gram of the adsorbent) because of the high loading of the incorporated isocyanurate bridging group and the large distribution coefficients (on order of 10^8) for mercury adsorption on these materials. Burleigh et al. [88] synthesized amine-functionalized PMOs by co-condensation of bis(triethoxysilyl) ethane and N-(2-aminoethyl)-3-aminopropyltrimethoxysilane (AAPTS). Adsorption of

Scheme 18 The chemical reaction catalyzed by amine-functionalized PMOs

Knoevenagel reaction

Cyanosilylation reaction

Claisen–Schmidt condensation

Cu(II)/trizma complexes from aqueous solutions indicates that more than 70% of these functional ligands are accessible for further reaction.

As to isocyanurate-bridged PMOs with high loadings of pendant thiol groups, synthesized via co-condensation of mercaptopropyl-containing silane and isocyanurate-containing silsesquioxane [228], both the bridging isocyanurate (ICS) groups and the pendant thiol groups can adsorb Hg^{2+}. Nevertheless, a small portion of the bridged ICS groups are at the pore surface and accessible to guest species. Therefore, only a small portion of the bridged ICS groups are chemically active in possible adsorption reaction, while a large portion of them are cross-linked to form the condensed frameworks to support the mesoporous structures, and these groups would not be engaged in reaction. However, the adsorption capacity of mercapto-functionalized ICS-PMOs are greater than the total adsorption capacities reported for thiol-modified mesoporous silica and ICS-PMOs with comparable amounts of incorporated ligands [229].

4.3 Application in biology

The adsorption of biomolecules onto inorganic–organic hybrid materials has attracted much attention, particularly because mesoporous materials are ideal solids for enzyme immobilization due to their high surface area, ordered and tunable pore size and reusability. Moreover, the surface or framework functionalization in PMOs make much viable to enhance the interaction of biomolecules and PMOs surface [230].

The principal driving forces in the adsorption of biomolecules onto porous hosts mainly include the electrostatic, hydrophobic (weak van der Waals), and hydrogen-bonding interaction [231]. PMOs with organic groups as an integrated part of the mesoporous wall may act as a unique host material for enzyme immobilization [232, 233]. The adsorption of lysozyme (Lz) as a model enzyme on silica or PMOs is determined by several factors. The adsorption capacity of Lz on ethane-PMO was lower than that of pure mesoporous silica and the electrostatic interaction is more dominant than the hydrophobic interaction in the bioadsorption of protein, probably due to the relatively weak interaction between the enzyme molecule and $–CH_2CH_2–$ in the mesoporous wall of PMOs. Li et al. have investigated the enzyme adsorption behavior of PMOs with various fractions of 1,4-diethylenebenzene and ethane bridging groups in the mesoporous wall [234]. It has been found that the amounts of adsorbed Lz depend on the surface characteristics and the textural properties of the mesoporous organosilicas and the solution pH. The maximum Lz adsorption amount of 360 mg g^{-1} has been achieved on bifunctional PMOs. Bifunctional PMOs with a fraction of 1,4-diethylenebenzene

in the mesoporous wall exhibits much higher adsorption capacity for Lz than PMOs with only the ethane moiety in the mesoporous wall. This is probably due to the fact that the 1,4-diethylenebenzene has stronger hydrophobic and hydrogen-bonding interactions with Lz than ethane.

A rapid, large-scale refolding of recombinant proteins from inclusion bodies is important in view of both fundamental studies and bioengineering applications. The formation of inactive protein aggregates, which competes with correct folding especially at high concentration, has been recognized as the main reason for inefficient protein recovery [235]. Batch dilution, as the most widely used and simplest approach, is usually carried out at a very low protein concentration (e.g., <0.1 mg/mL). Wang et al. reported a new methodology for protein refolding by the controlled release of unfolded proteins from ordered mesoporous materials without disturbing the optimal refolding condition [236]. As illustrated in Scheme 19, the new protein refolding strategy takes advantage of the unique surface and structural properties of PMOs, which can effectively entrap denatured proteins and exhibit a stimuli-responsive controlled release of entrapped proteins into the refolding buffer. Through the loading of denatured proteins inside uniform mesoporous channels tailored to accommodate individual proteins, protein aggregation is minimized and the continuous release of denatured proteins ensures cumulative refolding. In addition, Poly(ethylene glycol) (PEG) was selected as a trigger to release encapsulated Lz from the mesopores because it can form strong H bonds with the silanol groups on the silica surface and thus reduce the affinity between Lz and PMOs. Subsequently, the elution rate, total amount, and concentration of Lz can be controlled by tuning the PEG concentration. Moreover, larger molecular weight of PEG leads to a faster release rate. This new strategy enables high-yield refolding at higher concentrations (e.g., >1 mg/mL) and can be extended to the refolding of other proteins. In addition, surface-functionalized silica nanoparticles can also deliver DNA into animal cells and tissues [237], and this ideal is being extended to the application of PMOs.

4.4 Application in analytical chemistry

High-performance liquid chromatography (HPLC) is currently a common technique for separating and analyzing multi-component mixtures [238]. More than 60% of all HPLC separations are carried out under reversed phase (RP) conditions. The application of stationary phases based on PMOs in HPLC is attractive with novelty [239, 240] because the separating properties of PMOs combine those of a normal and a reversed phase through the combination of silanol groups and organic bridges in the framework. Before, the surface modification of well defined silica
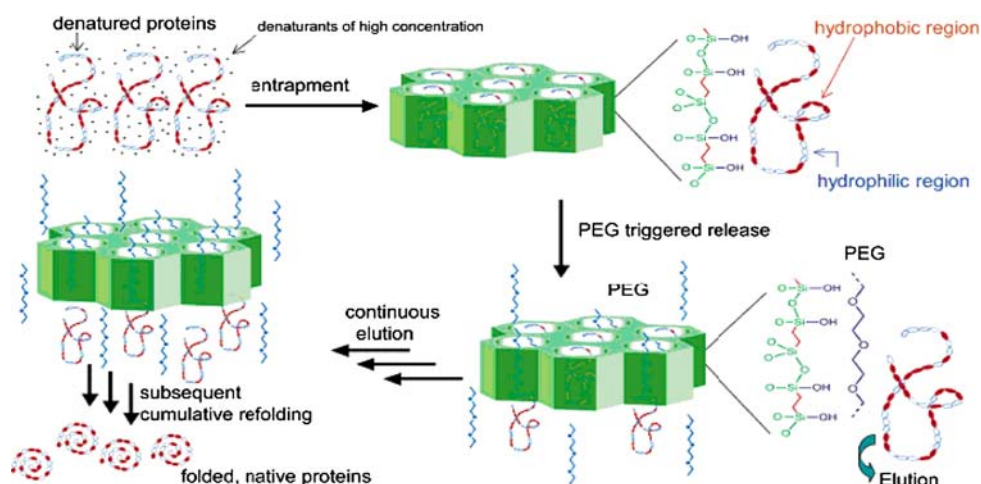
beads by introducing terminal or bridged functionalized organic groups is the major route to creating phases for reversed phase liquid chromatography (RPLC) [241, 242]. Recently, spherical PMOs (sph-PMOs) have been synthesized by utilization of the modified Stoeber reaction [243] or microwave heating method [244]. One of the most exciting potential applications of spherical PMOs is as a stationary phase in HPLC [245, 246]. Kim et al. [242] have prepared PMOs containing uniform ethane groups in the pore walls using microwave heating to produce 1.5–2.5-mm uniform particles with spherical morphology. These materials demonstrated improvements as HPLC column materials over the conventionally prepared PMOs [45]. In this aspect, it is desirable that PMOs spheres are monodispersed and of a size no lower than 2–3 μm so as to allow easy packing and reduce hydrodynamic energy costs [181].

PMOs with functional organic molecules incorporated into the structure offer another potential to provide detection capabilities as chemical sensors [247]. The porphyrin macrocycle consists of 22 π-electrons, resulting in a high degree of sensitivity to chemical structure of cyclic organic molecules relative to a wide range of optical detection [248, 249]. Recently, porphyrin-embedded PMOs have been used to detect explosive organics such as TNT (2,4,6-trinitrotoluene) over the other analytes (p-nitrophenol, p-cresol, 2,4,6-trinitrotoluene and cyclotrimethylenetrinitramine) with high selectivity [250]. The binding of each of these organic molecules by the porphyrin-embedded PMOs results in unique changes in the spectrophotometric characteristics of the incorporated porphyrin. Consequently, the qualitative and quantitative analysis of each chemical can be achieved [250, 251].

Another interesting application in chemical analysis is that of PMOs doped with rare-earth ions such as Eu^{3+}, Tb^{3+} and Tm^{3+}, which can be served as a UV sensor. The unique optical property of rare-earth ions doped in a host material makes it very important in UV sensor application.

PMOs with uniform mesopores, high surface area, and good thermal and chemical stability, can be a potential host. Park et al. [252] synthesized transparent and oriented PMO monoliths with doping rare-earth ions (Eu^{3+}, Tb^{3+} and Tm^{3+}) into the materials. By photoluminescence spectra, it was found that Eu^{3+}-, Tb^{3+}- and Tm^{3+}-doped PMOs monoliths exhibited interesting UV sensing characteristics and produced red-, green- and blue-emission upon UV irradiation with the characteristic emission peaks. Moreover, intensity of photoluminescence peaks of the rare-earth ion-doped PMOs monoliths increased with increasing the rare-earth ion contents.

4.5 Application in microelectronics

There is a growing interest in low dielectric materials, which can be used to increase the effective capacitance between metal interconnections in semiconductor devices. Ideal dielectric materials must have properties of: high porosity (the low dielectric constant of air $k = 1$), mechanical and thermal stability, and minimal moisture absorption [253, 254]. There have been some studies of bulk mesoporous inorganic and organic hybrids silica with low dielectric constant, either as xerogels or pore generator-templated solids, prior to PMOs [255–257]. Hydrophobic organosilicas are more promising matrix materials for ultra low-k dielectrics compared to pure silica materials [258].

To fabricate PMOs with low dielectric constant, Lu et al. [127] have reported an evaporation-induced self-assembly procedure to prepare poly(bridged silsesquioxane) thin-film and particulate mesophases that incorporate organic moieties(ethane, methylene, benzene) into periodic, mesostructured frameworks as molecularly dispersed bridging ligands. A consistent trend of increasing modulus (E) and hardness (H) and decreasing dielectric constant was observed with substitution of the bridged silsesquioxane for siloxane in the framework. Hatton et al. have produced thin film PMOs via

an evaporation-induced self-assembly spin-coating procedure using silsequioxanes of the type $(C_2H_5O)_3Si$-R-$Si(OC_2H_5)_3$ or R'-$[Si(OC_2H_5)_3]_3$ with R = methene(-CH_2-), ethylene(-CH_2CH_2), 1,4-phenylene (C_6H_4), and R' = 1,3,5-phenylene(C_6H_3) as organosilica precursors [259]. The dielectric constant (k) of these materials was found decreased for the film which was thermally treated to bring about a "self-hyrhophobizing" bridging-to-terminal transformation (e.g., bridging methylene groups -CH_2- transform to terminal methyl groups -CH_3 [31]). The resistance to moisture adsorption also is enhanced by increasing the organic content and thermal treatment. As to such PMOs, the trend of increasing mechanical and thermal stability and decreasing dielectric constant is of crucial interest to the burgeoning field of low-*k* dielectrics.

5 Conclusions

In the past decade, the rapid growth in development of PMOs with various organic groups in the framework allows one to finely tune the properties of PMOs to achieve the desired multifunctionalilties and applications. The syntheses of PMOs can be carried out (1) by one-pot hydrolysis and co-condensation from inorganic precursors and bridged organosiloxane precursors, the bridged organosiloxane precursors with terminal organosiloxane precursors, (2) by co-condensation of multiple bridged organosiloxane precursors in the presence of supramolecular structure-directing agents, or (3) by two-step post-synthesis. The physical and chemical properties of PMOs depend on the composition of the bridge-bonded silsesquioxane precursor and various synthesis parameters such as the type of surfactant, additive, pH, presence or absence of cosurfactants, counter ions, temperature, concentrations, geometry of the organic unit (rigid, flexible, trifunctional), and the ionic strength of the solution. While the wide range of variables may seem to make accurate control of PMOs elusive, such variables in the process of synthesizing PMOs provide many possible routes to engineering varied structures and properties of PMOs. Theoretically, there are enormous possibilities to deliberately tune the chemical and physical properties of the PMOs by varying the organic spacer groups of the organosilica precursors and the synthesis parameters. Previous results in the literature have shown that the proper choice of the silsesquioxane precursors and synthesizing conditions is an effective method for improving the ordering of mesostructure and hydrothermal and chemical stability.

Despite the remarkable progress in the synthesis chemistry of PMOs, many challenges still exist to obtain PMOs with ideal mesostructured ordering, stability and multifunctional properties. Regarding synthetic systems, the organosilica systems possess fewer sites (e.g., hydroxyl groups or protonated hydroxyl groups) interacting with template in comparison with the pure-silica synthetic systems. Consequently, the initial organosilicate-template condensation and assembly is relatively poorly organized compared with mesoporous silica systems. Moreover, bridge-bonded organic units have less flexibility, so bridged silsesquioxanes generally do not form as good replications of the micelle template compared to silicas. To date, the precursors used for the synthesis of PMOs normally consist of short aliphatic chains or symmetrical aryl bridging groups. Still, limited types of organosilica precursors have been successfully converted into PMOs. Another challenge is that real crystalline PMOs have not yet been obtained. Further attempts should be undertaken to develop more compatible and economic methods which are applicable for the synthesis of PMOs with more functional and even more complicated bridge-bonded organic groups at desire.

As summarized above, the potentials of PMOs have been tested in the fields of catalysis, adsorption and separation, biological techniques and electronic devices. Many results look much positive. Nevertheless, much research is still in the early stages. There exists still many opportunities to improve the properties and functionalities of PMOs and to apply them to lots of new fields. Undoubtedly, with further knowledge of synthesis chemistry and correlation of structure and properties, there is a promising future of both scientific significance and great commercial value for PMOs with narrow pore-size distribution, highly ordered structure, and homogeneously distributed functional organic and inorganic groups.

References

1. C.T. Kresge, M.E. Leonowicz, W.J. Roth, J.C. Vartuli, J.S. Beck, Nature **359**, 710 (1992). doi:10.1038/359710a0
2. S. Inagaki, Y. Fukushima, K. Kuroda, J. Chem. Soc. Chem. Commun. **680** (1993). doi:10.1039/c39930000680
3. Q. Huo, R. Leon, P.M. Petroff, G.D. Stucky, Science **268**, 1324 (1995). doi:10.1126/science.268.5215.1324
4. D. Zhao, Q. Huo, J. Feng, J. Kim, Y. Han, G.D. Stucky, Chem. Mater. **11**, 2668 (1999). doi:10.1021/cm980755t
5. P.T. Tanev, T.J. Pinnavaia, Science **267**, 865 (1995). doi:10.1126/science.267.5199.865
6. S.A. Bagshaw, E. Prouzet, T.J. Pinnavaia, Science **269**, 1242 (1995). doi:10.1126/science.269.5228.1242
7. S.S. Kim, W. Zhang, T.J. Pinnavaia, Science **282**, 1302 (1998). doi:10.1126/science.282.5392.1302
8. R. Ryoo, J.M. Kim, C.H. Ko, C.H. Shin, J.Y. Lee, J. Phys. Chem. **100**, 17718 (1996). doi:10.1021/jp9620835

9. Y.P. Zhang, C.H. Zhou, X.J. Wang, T. Yong, Y.Z. Xu, Prog. Chem. **20**, 33 (2008)

10. S.L. Burkett, S.D. Sims, S. Mann, Chem. Commun. (Camb) 1367 (1996) doi:10.1039/cc9960001367

11. D.J. Macquarrie, Chem. Commun. (Camb) 1961 (1996). doi:10.1039/cc9960001961

12. M.E. Lim, C.F. Blanford, A. Stein, Chem. Mater. **10**, 467 (1998). doi:10.1021/cm970713p

13. C.E. Fowler, S.L. Burkett, S. Mann, Chem. Commun. (Camb) 1769, (1997). doi:10.1039/a704644h

14. K. Moller, T. Bein, Chem. Mater. **10**, 2950 (1998). doi:10.1021/cm980243e

15. B.J. Melde, B.T. Holland, C.F. Blanford, A. Stein, Chem. Mater. **11**, 3302 (1999). doi:10.1021/cm9903935

16. T. Asefa, M.J. MacLachlan, N. Coombs, G.A. Ozin, Nature **402**, 867 (1999)

17. T. Asefa, C. Yoshina-Ishii, M.J. MacLachlan, G.A. Ozin, J. Mater. Chem. **10**, 1751 (2000). doi:10.1039/b000950o

18. O. Dag, C. Yoshina-Ishii, T. Asefa, M.J. MacLachlan, H. Grondley, N. Coombos, G.A. Ozin, Adv. Funct. Mater. **11**, 213 (2001). doi:10.1002/1616-3028(200106)11:3<213::AID-ADFM 213>3.0.CO;2-C

19. X.Y. Bao, X.S. Zhao, J. Phys. Chem. B **109**, 10727 (2005). doi:10.1021/jp050449k

20. W.J. Hunks, G.A. Ozin, J. Mater. Chem. **15**, 3716 (2005). doi:10.1039/b504511h

21. W. Whitnall, T. Asefa, G.A. Ozin, Funct. Mater. **15**, 1696 (2005). doi:10.1002/adfm.200500151

22. B. Hatton, K. Landskron, W. Whitnall, D. Perovic, G.A. Ozin, Acc. Chem. Res. **38**, 305 (2005). doi:10.1021/ar040164a

23. J. Patarin, B. Lebeau, R. Zana, Curr. Opin. Colloid Sci. **7**, 107 (2002). doi:10.1016/S1359-0294(02)00012-2

24. K. Yamarnoto, T. Tatsumi, Chem. Mater. **20**, 972 (2008). doi:10.1021/cm7028646

25. P. Van der Voort, C. Vercaemst, Phys. Chem. Chem. Phys. **10**, 347 (2008). doi:10.1039/b707388g

26. F. Hoffmann, M. Cornelius, J. Morell, M. Froba, J. Nanosci. Nanotechnol. **2**, 6 (2006)

27. F. Hoffmann, M. Cornelius, J. Morell, M. Froba, Angew. Chem. Int. Ed. **20**, 45 (2006)

28. S. Inagaki, S. Guan, Y. Fukushima, Chem. Soc. **121**, 9611 (1999). doi:10.1021/ja9916658

29. K. Landskron, B.D. Hatton, D.D. Perovic, G.A. Ozin, Science **302**, 266 (2003). doi:10.1126/science.1084973

30. R.M. Grudzien, E.G. Bogna, M. Jaroniec, J. Mater. Chem. **16**, 819 (2006). doi:10.1039/b515975j

31. T. Asefa, M.J. MacLachlan, H. Grondey, N. Coombs, G.A. Ozin, Metamorphic channels in periodic mesoporous methylenesilica. Angew. Chem. Int. Ed. **39**, 1808 (2000). doi:10.1002/(SICI)1521-3773(20000515)39:10<1808::AID-ANIE1808>3.0.CO;2-G

32. M.C. Burleigh, M.A. Markowitz, S. Jayasundera, M.S. Spector, C.W. Thomas, B.P. Gaber, J. Phys. Chem. B **107**, 12628 (2003). doi:10.1021/jp035189q

33. E.B. Cho, K. Char, Chem. Mater. **16**, 270 (2004). doi:10.1021/cm0346733

34. Y. Goto, S. Inagaki, Chem. Commun. (Camb) 2410 (2002). doi:10.1039/b207825b

35. M.P. Kapoor, S. Inagaki, S. Ikeda, K. Kakiuchi, M. Suda, T. Shimada, J. Am. Chem. Soc. **127**, 8174 (2005). doi:10.1021/ja043062o

36. A. Sayari, W. Wang, J. Am. Chem. Soc. **127**, 12194 (2005). doi:10.1021/ja054103z

37. G. Temtsin, T. Asefa, S. Bittner, G.A. Ozin, J. Mater. Chem. **11**, 3202 (2001). doi:10.1039/b103960c

38. E.B. Cho, D. Kim, Chem. Lett. **36**, 118 (2007). doi:10.1246/cl.2007.118

39. B. Boury, R.J.P. Corriu, Chem. Commun. (Camb) 795 (2002). doi:10.1039/b109040m

40. M.P. Kapoor, Q. Yang, S. Inagaki, J. Am. Chem. Soc. **124**, 15176 (2002). doi:10.1021/ja0290678

41. M. Kuroki, T. Asefa, W. Whitnal, M. Kruk, C. Yoshina-Ishii, M. Jaroniec, G.A.J. Ozin, Am. Chem. Soc. **124**, 13886 (2002). doi:10.1021/ja027877d

42. W.J. Hunks, G.A. Ozin, Chem. Commun. (Camb) 2426 (2004). doi:10.1039/b410397a

43. O. Olkhovyk, M. Jaroniec, J. Am. Chem. Soc. **127**, 60 (2005). doi:10.1021/ja043941a

44. H.W. Oviatt, K.J. Shea, J.H. Small, Chem. Mater. **5**, 943 (1993). doi:10.1021/cm00031a012

45. S. Guan, S. Inagaki, T. Ohsuna, O. Terasaki, J. Am. Chem. Soc. **122**, 5660 (2000). doi:10.1021/ja000839e

46. C.J. Brinker, G.W. Scherer, *Sol–Gel Science – The Physics and Chemistry of Sol–Gel Processing* (Academic Press, London, 1990), pp. 97–234

47. J.M. Kim, Y.J. Han, B.F. Chmelka, G.D. Stucky, Chem. Commun. (Camb) 2437 (2000). doi:10.1039/b005608l

48. X.Y. Bao, X.S. Zhao, X. Li, P.A. Chia, J. Li, J. Phys. Chem. B **108**, 4684 (2004). doi:10.1021/jp037342m

49. D. Dube, M. Rat, F. Beland, S. Kaliaguine, Microporous Mesoporous Mater. **111**, 596 (2008). doi:10.1016/j.micromeso.2007.09.005

50. M.H. Lim, C.F. Blanford, A. Stein, J. Am. Chem. Soc. **119**, 4090 (1997). doi:10.1021/ja9638824

51. R.M. Grudzien, B.E. Grabicka, M. Jaroniec, Colloids Surf. A Physchem. Eng. Aspects **300**, 235 (2007)

52. C. Yoshina-Ishii, T. Asefa, N. Coombs, M.J. MacLachlan, G.A. Ozin, Chem. Commun. (Camb) 2539 (1999). doi:10.1039/a908252b

53. K. Landskron, G.A. Ozin, Angew. Chem. Int. Ed. **44**, 2107 (2005). doi:10.1002/anie.200462279

54. G. Cerveau, R.J.P. Corriu, E. Framery, F. Lerouge, Chem. Mater. **16**, 3794 (2004). doi:10.1021/cm049061c

55. J.J.E. Moreau, L. Vellutini, C. Bied, J. Am. Chem. Soc. **123**, 1509 (2001). doi:10.1021/ja003843z

56. G. Cerveau, R.J.P. Corriu, F. Lerouge, N. Bellec, D. Lorcy, M. Nobili, Chem. Commun. (Camb) 396 (2004). doi:10.1039/b314262k

57. T. Kishida, N. Fujita, K. Sada, S. Shinkai, Langmuir **21**, 9432 (2005). doi:10.1021/la0515569

58. K. Okamoto, Y. Goto, S. Inagaki, J. Mater. Chem. **15**, 4136 (2005). doi:10.1039/b508818f

59. S. Fujita, S. Inagaki, Chem. Mater. **20**, 891 (2008). doi:10.1021/cm702271v

60. S. Inagaki, S. Guan, T. Ohsuna, O. Terasaki, Nature **406**, 304 (2002). doi:10.1038/416304a

61. W.J. Hunks, G.A. Ozin, Chem. Mater. **16**, 5465 (2004). doi:10.1021/cm048986p

62. Y. Yang, A. Sayari, Chem. Mater. **19**, 4117 (2007). doi:10.1021/cm071258s

63. M.P. Kapoor, Q. Yang, S. Inagaki, Chem. Mater. **16**, 1209 (2004). doi:10.1021/cm034898d

64. Y. Luo, P.P. Yang, Microporous Mesoporous Mater. **111**, 194 (2008). doi:10.1016/j.micromeso.2007.07.029

65. N.K. Mal, M. Fujiwara, Y. Tanaka, Nature **421**, 350 (2003). doi:10.1038/nature01362

66. J. Morell, G. Wolter, M. Froba, Chem. Mater. **17**, 804 (2005). doi:10.1021/cm048302d

67. G. Dubois, R.J.P. Corriu, C. Reye, S. Brandès, F. Denat, R. Guilard, Chem. Commun. (Camb) 2283 (1999). doi:10.1039/a907217i

68. C. Chuit, R.J.P. Corriu, G. Dubois, C. Reye, Chem. Commun. (Camb) 723 (1999). doi:10.1039/a900767i
69. G. Dubois, C. Reye, C. Chuit, R.J.P. Corriu, J. Mater. Chem. **10**, 1091 (2000). doi:10.1039/a909201c
70. R.J.P. Corriu, A. Mehdi, C. Reye, C. Thieuleux, Chem. Commun. (Camb) 1382 (2002). doi:10.1039/b202179j
71. R.M. Grudzien, S. Pikus, M. Jaroniec, J. Phys. Chem. B **110**, 2972 (2006). doi:10.1021/jp0574652
72. C.Q. Liu, H.T. Zhao, P. Xie, R.B. Zhang, J. Polym. Sci. A **38**, 2702 (2000). doi:10.1002/1099-0518(20000801)38:15<2702::AID-POLA100>3.0.CO;2-4
73. L. Zhang, W. Zhang, J. Shi, Z. Hua, Y. Li, J. Yan, Chem. Commun. (Camb) 210 (2003). doi:10.1039/b210457a
74. J.J.E. Moreau, B.P. Pichon, M.W.C. Man, C. Bied, H. Pritzkow, J.L. Bantignies, P. Dieudonne, J.L. Sauvajol, Angew. Chem. Int. Ed. **43**, 203 (2004). doi:10.1002/anie.200352485
75. J.N. Li, T. Qi, L. Wang, Y. Zhou, C.H. Liu, Y. Zhang, Microporous Mesoporous Mater. **103**, 184 (2007). doi:10.1016/j.micromeso.2007.01.038
76. C. Li, H.D. Zhang, D.M. Jiang, Q.H. Yang, Chem. Commun. (Camb) 547 (2007). doi:10.1039/b609862b
77. J. Morell, S. Chatterjee, P.J. Klar, D. Mauder, I. Shenderovich, F. Hoffmann, M. Froba, Chem. Eur. J. **14**, 5935 (2008). doi:10.1002/chem.200800239
78. D.M. Jiang, Q.H. Yang, H. Wang, G.R. Zhu, J. Yang, C. Li, J. Catal. **239**, 65 (2006). doi:10.1016/j.jcat.2006.01.018
79. C. Baleizao, B. Gigante, D. Das, M. Alvaro, H. Garcia, A. Corma, Chem. Commun. (Camb) 1860 (2003). doi:10.1039/b304814d
80. S. Polarz, A. Kuschel, Adv. Mater. **18**, 1206 (2006). doi:10.1002/adma.200502647
81. A. Ide, R. Voss, G. Scholz, G.A. Ozin, M. Antonietti, A. Thomas, Chem. Mater. **19**, 2649 (2007). doi:10.1021/cm063026j
82. C.C. Wang, W. Shan, Y. Zhang, N. Ren, W. Yang, Y. Tang, Angew. Chem. Int. Ed. **45**, 2088 (2006). doi:10.1002/anie.200504191
83. S. Yang, L. Zhao, C. Yu, X. Zhou, J. Tang, P. Yuan, D. Chen, D. Zhao, J. Am. Chem. Soc. **128**, 10460 (2006). doi:10.1021/ja0619049
84. X.J. Meng, T. Yokoi, D.L. Lu, T. Tatsumi, Angew. Chem. Int. Ed. **46**, 7796 (2007). doi:10.1002/anie.200702666
85. Y.P. Zhang, C.H. Zhou, J.H. Fei, Y.M. Yu, X.M. Zheng, J. Mol. Catal. **21**, 109 (2007)
86. W.H. Zhang, B. Daly, J. O'Callaghan, L. Zhang, J.L. Shi, C. Li, M.A. Morris, J.D. Holmes, Chem. Mater. **17**, 6407 (2005). doi:10.1021/cm050502h
87. M.C. Burleigh, S. Dai, E.W. Hagaman, J.S. Lin, Chem. Mater. **13**, 2537 (2001). doi:10.1021/cm000894m
88. M.C. Burleigh, M.A. Markowitz, M.S. Spector, B.P. Gaber, Chem. Mater. **13**, 4760 (2001). doi:10.1021/cm0105763
89. M.C. Burleigh, M.A. Markowitz, M.S. Spector, B.P. Gaber, J. Phys. Chem. B **105**, 9935 (2001). doi:10.1021/jp011814k
90. D. Coutinho, C.R. Xiong, K.J. Balkus, Microporous Mesoporous Mater. **108**, 86 (2008). doi:10.1016/j.micromeso.2007.03.030
91. Q. Yang, M.P. Kapoor, S. Inagaki, J. Am. Chem. Soc. **124**, 9694 (2002). doi:10.1021/ja026799r
92. Q.H. Yang, H. Liu, H. Yang, L. Zhang, Z.C. Feng, J. Zhang, C. Li, Microporous Mesoporous Mater. **77**, 257 (2005). doi:10.1016/j.micromeso.2004.09.009
93. S. Shylesh, P.P. Samuel, C. Srilakshmi, R. Parischa, A.P. Singh, J. Mol. Catal. Chem. **274**, 153 (2007). doi:10.1016/j.molcata.2007.04.040
94. Q.H. Yang, M.P. Kapoor, S. Inagaki, N. Shirokura, J.N. Kondo, K. Domen, J. Mol. Catal. Chem. **230**, 85 (2005). doi:10.1016/j.molcata.2004.12.010
95. S. Hamoudi, S. Kaliaguine, Microporous Mesoporous Mater. **59**, 195 (2003)
96. B. Rac, P. Hegyes, P. Forgo, A. Molnar, Appl. Catal. A Gen. **299**, 193 (2006)
97. Q.H. Yang, M.P. Kapoor, N. Shirokura, M. Ohashi, S. Inagaki, J.N. Kondo, K. Domen, J. Mater. Chem. **15**, 666 (2005). doi:10.1039/b413773f
98. S. Hamoudi, S. Royer, P. Forgo, A. Molnar, Microporous Mesoporous Mater. **71**, 17 (2004). doi:10.1016/j.micromeso.2004.03.009
99. T. Asefa, M. Kruk, M.J. MacLachlan, N. Coombs, H. Grondey, M. Jaroniec, G.A. Ozin, J. Am. Chem. Soc. **123**, 8520 (2001). doi:10.1021/ja0037320
100. M.C. Burleigh, S. Jayasundera, M.S. Spector, C.W. Thomas, M.A. Markowitz, B.P. Gaber, Chem. Mater. **16**, 3 (2004). doi:10.1021/cm034862l
101. Y.Z. Khimyak, J. Klinowski, Phys. Chem. Chem. Phys. **3**, 616 (2001). doi:10.1039/b007473j
102. J.T.A. Jones, C.D. Wood, C. Dickinson, Y.Z. Khimyak, Chem. Mater. **20**, 3385 (2008). doi:10.1021/cm7036124
103. B.A. Treuherz, Y.Z. Khimyak, Microporous Mesoporous Mater. **106**, 236 (2007). doi:10.1016/j.micromeso.2007.03.005
104. W.H. Zhang, X.N. Zhang, Z. Hua, P. Harish, F. Schroeder, S. Hermes, T. Cadenbach, Chem. Mater. **19**, 2663 (2007). doi:10.1021/cm061922p
105. R.M. Grudzien, B.E. Grabicka, S. Pikus, M. Jaroniec, Chem. Mater. **18**, 1722 (2006). doi:10.1021/cm052717x
106. J. Morell, M. Gungerich, G. Wolter, J. Jiao, M. Hunger, P.J. Klar, M. Froba, J. Mater. Chem. **16**, 2809 (2006). doi:10.1039/b603458f
107. Y. Guo, A. Mylonakis, Z.T. Zhang, P.I. Lelkes, K. Levon, S.X. Li, Q.W. Feng, Y. Wei, Macromolecules **40**, 2721 (2007). doi:10.1021/ma0622985
108. D.M. Jiang, Q.H. Yang, J. Yang, L. Zhang, G.R. Zhu, W.G. Su, C. Li, Chem. Mater. **17**, 6154 (2005). doi:10.1021/cm0514084
109. M. Alvaro, B. Ferrer, H. Garcia, F. Rey, Chem. Commun. (Camb.) **18**, 2012 (2002). doi:10.1039/b205883a
110. H.G. Zhu, D.J. Jones, J. Zajac, R. Dutartre, M. Rhomari, J. Roziere, Chem. Mater. **14**, 4886 (2002). doi:10.1021/cm011742+
111. S. Jayasundera, M.C. Burleigh, M. Zeinali, M.S. Spector, J.B. Miller, W.F. Yan, S. Dai, M.A. Markowitz, J. Phys. Chem. B **109**, 9198 (2005). doi:10.1021/jp051435h
112. E.B. Cho, D. Kim, M. Jaroniec, Langmuir **23**, 11844 (2007). doi:10.1021/la701948g
113. E.B. Cho, D. Kim, Microporous Mesoporous Mater. **113**, 530 (2008). doi:10.1016/j.micromeso.2007.12.010
114. A.E.C. Palmqvist, Curr. Opin. Colloid Interface Sci. **8**, 145 (2003). doi:10.1016/S1359-0294(03)00020-7
115. Y.C. Liang, E.S. Erichsen, M. Hanzlik, R. Anwander, Chem. Mater. **20**, 1451 (2008). doi:10.1021/cm702359r
116. Q. Huo, D.I. Margolese, U. Ciesla, D.G. Demuth, P. Feng, T.E. Gier, P. Sieger, A. Firouzi, B.F. Chmelka, F. Schuth, G.D. Stucky, Chem. Mater. **6**, 1176 (1994). doi:10.1021/cm00044a016
117. C.Z. Yu, J. Fan, B.Z. Tian, D.Y. Zhao, Chem. Mater. **16**, 889 (2004). doi:10.1021/cm035011g
118. P.V. Braun, P. Osenar, S.I. Stupp, Nature **380**, 325 (1996). doi:10.1038/380325a0
119. C.J. Brinker, D.R. Dunphy, Curr. Opin. Colloid Interface Sci. **11**, 126 (2006). doi:10.1016/j.cocis.2005.10.006
120. Y.D. Xia, R. Mokaya, J. Phys. Chem. B **110**, 3889 (2006). doi:10.1021/jp055548c
121. A. Sayari, S. Hamoudi, Y. Yang, I.L. Moudrakowski, J.R. Ripmeester, Chem. Mater. **12**, 3857 (2000). doi:10.1021/cm000479u

122. S. Hamoudi, Y. Yang, I.L. Moudrakovski, S. Lang, A. Sayari, J. Phys. Chem. B **105**, 9118 (2001). doi:10.1021/jp011195f

123. Z.R.R. Tian, J. Liu, J.A. Voigt, H.F. Xu, M.J. Mcdermot, Nano Lett. **3**, 89 (2003). doi:10.1021/nl025828t

124. Y.C. Liang, M. Hanzlik, R. Anwander, Chem. Commun. (Camb) 525 (2005). doi:10.1039/b411146j

125. Y.C. Liang, M. Hanzlik, R. Anwander, J. Mater. Chem. **15**, 3919 (2005). doi:10.1039/b504600a

126. A. Sayari, Y. Yang, Chem. Commun. (Camb) 2582 (2002). doi:10.1039/b208512g

127. Y. Lu, H. Fan, N. Doke, D.A. Loy, R.A. Assink, D.A. LaVan, C.J. Brinker, J. Am. Chem. Soc. **122**, 5258 (2000). doi:10.1021/ja9935862

128. H. Fan, S. Reed, T. Baer, R. Schunk, G.P. Lopez, C.J. Brinker, Microporous Mesoporous Mater. **625**, 44 (2001)

129. M.C. Burleigh, M.A. Markowitz, M.S. Spector, B.P. Gaber, J. Phys. Chem. B **106**, 9712 (2002). doi:10.1021/jp025515m

130. N. Bion, P. Ferreira, A. Valente, I.S. Goncüalves, J. Rocha, J. Mater. Chem. **13**, 1910 (2003). doi:10.1039/b304430k

131. M.C. Burleigh, S. Jayasundera, C.W. Thomas, M.S. Spector, M.A. Markowitz, B.P. Gaber, Colloid Polym. Sci. **282**, 728 (2004). doi:10.1007/s00396-003-1004-0

132. O. Dag, G.A. Ozin, Adv. Mater. **13**, 1182 (2001). doi:10.1002/1521-4095(200108)13:15<1182::AID-ADMA1182>3.0.CO;2-#

133. D. Zhao, Q. Huo, J. Feng, B.F. Chmelka, G.D. Stucky, J. Am. Chem. Soc. **120**, 6024 (1998). doi:10.1021/ja974025i

134. O. Muth, C. Schellbach, M. Froba, Chem. Commun. (Camb) 2032 (2001). doi:10.1039/b106636f

135. C. Booth, D. Attwood, C. Price, Phys. Chem. Chem. Phys. **8**, 3612 (2006). doi:10.1039/b605367j

136. C. Booth, D. Attwood, Macromol. Rapid Commun. **21**, 501 (2000). doi:10.1002/1521-3927(20000601)21:9<501::AID-MARC501>3.0.CO;2-R

137. C.Z. Yu, J. Fan, B.Z. Tian, G.D. Stucky, D.Y. Zhao, J. Phys. Chem. B **107**, 13368 (2003). doi:10.1021/jp027046u

138. E.B. Cho, K.W. Kwon, K. Char, Chem. Mater. **13**, 3837 (2001). doi:10.1021/cm010249v

139. O. Olkhovyk, M. Kruk, R. Sutton, M. Jaroniec, Nanoporous Mater. Iv **156**, 673 (2005). doi:10.1016/S0167-2991(05)80272-1

140. J.R. Matos, M. Kruk, L.P. Mercuri, M. Jaroniec, T. Asefa, N. Coombs, G.A. Ozin, T. Kamiyama, O. Terasaki, Chem. Mater. **14**, 1903 (2002). doi:10.1021/cm025513e

141. C. Yu, Y. Yu, D. Zhao, Chem. Commun. (Camb) 575 (2000). doi:10.1039/b000603n

142. Q.S. Huo, D.I. Margolese, G.D. Stucky, Chem. Mater. **8**, 1147 (1996). doi:10.1021/cm960137h

143. R. Ryoo, S.H. Joo, J.M. Kim, J. Phys. Chem. B **103**, 7435 (1999). doi:10.1021/jp9911649

144. Y.C. Liang, M. Hanzlik, R. Anwander, J. Mater. Chem. **16**, 1238 (2006). doi:10.1039/b514181h

145. M.P. Kapoor, S. Inagaki, Chem. Mater. **14**, 3509 (2002). doi:10.1021/cm020345b

146. Y. Muto, K. Esumi, K. Meguro, R. Zana, J. Colloid Interface Sci. **120**, 162 (1987). doi:10.1016/0021-9797(87)90335-3

147. Y. Han, D. Li, L. Zhao, J. Song, X. Yang, N. Li, C. Li, S. Wu, X. Xu, X. Meng, K. Lin, F.S. Xiao, Angew. Chem. Int. Ed. **42**, 3633 (2003). doi:10.1002/anie.200351466

148. H. Djojoputro, X.F. Zhou, S.Z. Qiao, L.Z. Wang, C.Z. Yu, G.Q. Lu, J. Am. Chem. Soc. **128**, 6320 (2006). doi:10.1021/ja0607537

149. M. Trau, N. Yao, E. Kim, Y. Xia, G.M. Whitesides, I.A. Aksay, Nature **390**, 674 (1997)

150. H. Miyata, K. Kuroda, Chem. Mater. **12**, 49 (2000). doi:10.1021/cm990506k

151. Z.R.R. Tian, J. Liu, H.F. Xu, J.A. Voigt, B. Mckenzie, C.M. Matzke, Nano Lett. **3**, 179 (2003). doi:10.1021/nl025900n

152. S.R. Zhai, I. Kim, C.S. Ha, J. Solid State Chem. **181**, 67 (2008). doi:10.1016/j.jssc.2007.11.011

153. S.R. Zhai, S.S. Park, M. Park, M.H. Uah, C.S. Ha, Microporous Mesoporous Mater. **113**, 47 (2008). doi:10.1016/j.micromeso.2007.11.001

154. B.L. Newalkar, S. Komarneni, Chem. Mater. **13**, 4573 (2001). doi:10.1021/cm0103038

155. D. Zhao, J. Sun, Q. Li, G.D. Stucky, Chem. Mater. **12**, 275 (2000). doi:10.1021/cm9911363

156. C. Yu, B. Tian, J. Fan, G.D. Stucky, D. Zhao, J. Am. Chem. Soc. **124**, 4556 (2002). doi:10.1021/ja025548f

157. W. Guo, J.Y. Park, M.O. Oh, H.W. Jeong, W.J. Cho, I. Kimand, C.S. Ha, Chem. Mater. **15**, 2295 (2003). doi:10.1021/cm0258023

158. S.Z. Qiao, C.Z. Yu, Q.H. Hu, Y.G. Jin, X.F. Zhou, X.S. Zhao, G.Q. Lu, Microporous Mesoporous Mater. **91**, 59 (2006). doi:10.1016/j.micromeso.2005.11.017

159. L. Zhang, H. Liu, H. Yang, Q.H. Yang, C. Li, Microporous Mesoporous Mater. **109**, 172 (2008). doi:10.1016/j.micromeso.2007.04.050

160. D.Y. Zhao, J.L. Feng, Q.S. Huo, N. Melosh, G.H. Fredrickson, B.F. Chmelka, G.D. Stucky, Science **279**, 5489 (1998)

161. K. Mortensen, J.S. Pedersen, Macromolecules **26**, 805 (1993). doi:10.1021/ma00056a035

162. W. Guo, I. Kim, C.S. Ha, Chem. Commun. (Camb) 2692 (2003). doi:10.1039/b308126e

163. E. Leontidis, Curr. Opin. Colloid Interface Sci. **7**, 81 (2002). doi:10.1016/S1359-0294(02)00010-9

164. K. Flodstrom, V. Alfredsson, N. Kallrot, J. Am. Chem. Soc. **125**, 4402 (2003). doi:10.1021/ja029353j

165. P. Alexandridis, J.F. Holzwarth, Langmuir **13**, 6074 (1997). doi:10.1021/la9703712

166. E.B. Cho, D. Kirn, Chem. Mater. **20**, 2468 (2008). doi:10.1021/cm702307s

167. J.M. Kim, S.K. Kim, R. Ryoo, Chem. Commun. (Camb) 259 (1998). doi:10.1039/a707677k

168. J.L. Blin, C. Otjacques, G. Herrier, B.-L. Su, Langmuir **16**, 4229 (2000). doi:10.1021/la9914615

169. Y.C. Liang, R. Anwander, Microporous Mesoporous Mater. **72**, 153 (2004). doi:10.1016/j.micromeso.2004.03.013

170. M.C. Burleigh, M.A. Markowitz, E.M. Wong, J.S. Lin, B.P. Gaber, Chem. Mater. **13**, 4411 (2001). doi:10.1021/cm010852d

171. L. Zhao, G.S. Zhu, D.L. Zhang, Y. Di, Y. Chen, O. Terasaki, S.L. Qiu, J. Phys. Chem. B **109**, 764 (2005). doi:10.1021/jp0465231

172. P. Schmidt-Winkel, P.D. Yang, D.I. Margolese, J.S. Lettow, J.Y. Ying, G.D. Stucky, Chem. Mater. **12**, 686 (2000). doi:10.1021/cm991097v

173. K. Nakanishi, Y. Kobayashi, T. Amatani, K. Hirao, T. Kodaira, Chem. Mater. **16**, 3652 (2004). doi:10.1021/cm049320y

174. W.H. Wang, S.H. Xie, W.Z. Zhou, A. Sayari, Chem. Mater. **16**, 1756 (2004). doi:10.1021/cm035235z

175. F. Kleitz, S.H. Choi, R. Ryoo, Chem. Commun. (Camb) 2136 (2003). doi:10.1039/b306504a

176. L. Mercier, T.J. Pinnavaia, Adv. Mater. **9**, 500 (1997). doi:10.1002/adma.19970090611

177. M.C. Burleigh, M.A. Markowitz, M.S. Spector, B.P. Gaber, Langmuir **17**, 7923 (2001). doi:10.1021/la011131w

178. F.S. Xiao, Curr. Opin. Colloid Interface Sci. **10**, 94 (2005). doi:10.1016/j.cocis.2005.05.006

179. X.F. Zhou, S.Z. Qiao, N. Hao, X.L. Wang, C.Z. Yu, L.Z. Wang, D.Y. Zhao, G.Q. Lu, Chem. Mater. **19**, 1870 (2007). doi:10.1021/cm062989f

180. C.H. Lee, S.S. Park, S.J. Choe, D.H. Park, Microporous Mesoporous Mater. **46**, 257 (2001). doi:10.1016/S1387-1811(01)00305-5

181. Y.D. Xia, R. Mokaya, J. Mater. Chem. **16**, 395 (2006). doi:10.1039/b511339c

182. A. Corma, H. Garcia, Adv. Syn. Cat. **348**, 1391 (2006). doi:10.1002/adsc.200606192

183. H.S. Xia, D.S. Tong, C.H. Zhou, G.F. Jiang, D. Zhang, Chi. Ind. Cat **16**, 8 (2008)

184. J. Li, C.H. Zhou, Z.X. Du, E.Z. Min, Z.H. Ge, X.N. Li, Prog. Chem. **19**, 444 (2007)

185. A. Fukuoka, Y. Sakamoto, S. Guan, S. Inagaki, N. Sugimoto, Y. Fukushima, K. Hirahara, S. Iijima, M. Ichikawa, J. Am. Chem. Soc. **123**, 3373 (2001). doi:10.1021/ja004067y

186. A. Fukuoka, H. Araki, Y. Sakamoto, S. Inagaki, Y. Fukushima, M. Ichikawa, Inorg. Chim. Acta **350**, 371 (2003). doi:10.1016/S0020-1693(02)01541-4

187. A. Corma, Chem. Rev. **97**, 2373 (1997). doi:10.1021/cr960406n

188. W.H. Yu, C.H. Zhou, Z.M. Ni, B. Zhang, Z.H. Ge, Chi. J. Cat. **27**, 961 (2006)

189. W.H. Yu, C.H. Zhou, Z.M. Ni, Z.H. Ge, Chem. Res. Chin. Univ. **23**, 127 (2007). doi:10.1016/S1005-9040(07)60026-9

190. W.H. Yu, C.H. Zhou, X.S. Xu, Z.H. Ge, Chi. Chem. Let. **18**, 341 (2007). doi:10.1016/j.cclet.2006.12.018

191. J.L. Shi, Z.L. Hua, L.X. Zhang, J. Mater. Chem. **14**, 795 (2004). doi:10.1039/b315861f

192. Y. Wan, D.Q. Zhang, Y.P. Zhai, C.M. Feng, J. Chen, H.X. Li, Chem. Asi. J. **2**, 875 (2007)

193. Y.C. Liang, R. Anwander, Dalton Trans. 1909 (2006). doi:10.1039/b516444c

194. A. Corma, D. Das, H. Garcia, A. Leyva, J. Catal. **229**, 322 (2005)

195. R.A. Garcia, R. van Grieken, J. Iglesias, V. Morales, D. Gordillo, Chem. Mater. **20**, 2964 (2008). doi:10.1021/cm703050u

196. C. Baleizao, B. Gigante, D. Das, M. Alvaro, H. Garcia, A. Corma, J. Catal. **223**, 106 (2004). doi:10.1016/j.jcat.2004.01.016

197. M. Alvaro, M. Benitez, D. Das, B. Ferrer, H. Garcia, Chem. Mater. **16**, 2222 (2004). doi:10.1021/cm0311630

198. M. Benitez, G. Bringmann, M. Dreyer, H. Garcia, H. Ihmels, M. Waidelich, K. Wissel, J. Org. Chem. **70**, 2315 (2005). doi:10.1021/jo047878j

199. D.M. Jiang, J.S. Gao, Microporous Mesoporous Mater. **113**, 385 (2008). doi:10.1016/j.micromeso.2007.11.036

200. W. Cho, J.W. Park, J. Li, Q.H. Yang, C. Li, Mater. Lett. **58**, 3551 (2004). doi:10.1016/j.matlet.2004.06.039

201. W. Guo, X.S. Zhao, Microporous Mesoporous Mater. **85**, 32 (2005). doi:10.1016/j.micromeso.2005.06.004

202. M.A. Wahab, C.S. Ha, J. Mater. Chem. **15**, 508 (2005). doi:10.1039/b412637h

203. S. Shylesh, C. Srilakshmi, A.P. Singh, B.G. Anderson, Microporous Mesoporous Mater. **99**, 334 (2007). doi:10.1016/j.micromeso.2006.09.029

204. S.R. Zhai, S.S. Park, M. Park, M.H. Ullah, C.S. Ha, Eur. J. Inorg. Chem. 5480 (2007). doi:10.1002/ejic.200700775

205. M. Vasconcellos-Dias, C.D. Nunes, P.D. Vaz, P. Ferreira, P. Brandao, V. Felix, M.J. Calhorda, J. Catal. **256**, 301 (2008)

206. S. Shylesh, A.P. Singh, Microporous Mesoporous Mater. **94**, 127 (2006). doi:10.1016/j.micromeso.2006.03.027

207. H.L. Xie, Y.X. Fan, C.H. Zhou, Z.X. Du, E.Z. Min, Z.H. Ge, X.N. Li, Chem. Biochem. Eng. Q. **22**, 25 (2008)

208. M.P. Kapoor, A.K. Sinha, S. Seelan, S. Inagaki, S. Tsubota, H. Yoshida, M. Haruta, Chem. Commun. (Camb) 2902 (2002). doi:10.1039/b209392h

209. J.A. Melero, J. Iglesias, J.M. Arsuaga, J. Mater. Chem. **17**, 377 (2007). doi:10.1039/b610868g

210. A. Bhaumik, M.P. Kapoor, S. Inagaki, Chem. Commun. (Camb) 470 (2003)

211. M.P. Kapoor, A. Bhaumik, S. Inagaki, J. Mater. Chem. **12**, 3078 (2002). doi:10.1039/b204524a

212. Z.H. Luan, C.F. Cheng, W.Z. Zhou, J. Klinowski, J. Phys. Chem. **99**, 1018 (1995). doi:10.1021/j100003a026

213. J.W. Kim, H.I. Lee, J.M. Kim, X. Yuan, J.E. Yie, Nanotechnol. Mesostruct. Mater. **146**, 665 (2003)

214. S. Shylesh, P.P. Samuel, A.P. Singh, Microporous Mesoporous Mater. **100**, 250 (2007). doi:10.1016/j.micromeso.2006.11.010

215. S.C. Laha, P. Mukherjee, S.R. Sainker, R. Kumer, J. Catal. **207**, 213 (2002). doi:10.1006/jcat.2002.3516

216. R. Savida, A. Panduragan, M. Palanchany, V. Murugesan, J. Mol. Catal. A **211**, 165 (2004). doi:10.1016/j.molcata.2003.10.022

217. Q. Yang, Y. Li, L. Zhang, H. Yang, J. Liu, C. Li, J. Phys. Chem. B **108**, 7934 (2004). doi:10.1021/jp040124o

218. X.D. Yuan, H.I. Lee, J.W. Kim, J.E. Yie, J.M. Kim, Chem. Lett. **32**, 650 (2003). doi:10.1246/cl.2003.650

219. Q. Yang, J. Liu, J. Yang, M.P. Kapoor, S. Inagaki, C. Li, J. Catal. **228**, 265 (2004)

220. R. Ballini, G. Bosica, J. Org. Chem. **62**, 425 (1997). doi:10.1021/jo961201h

221. R. Ballini, G. Bosica, P. Forconi, Tetrahedron **52**, 1677 (1996). doi:10.1016/0040-4020(95)00996-5

222. D.J. Macquarrie, D.B. Jackson, Chem. Commun. (Camb) **18**, 1781 (1997). doi:10.1039/a704156j

223. D.J. Macquarrie, Green Chem. **1**, 195 (1999). doi:10.1039/a904692e

224. M.L. Kantam, P. Sreekanth, P.L. Santhi, Green Chem. **2**, 47 (2000). doi:10.1039/a908758c

225. X. Wang, Y.H. Tseng, S. Cheng, J.C.C. Chan, J. Catal. **233**, 266 (2005)

226. M.C. Burleigh, M.A. Markowitz, M.S. Spector, B.P. Gaber, Environ. Sci. Technol. **36**, 2515 (2002). doi:10.1021/es011115l

227. T. Asefa, M. Kruk, N. Coombs, H. Grondey, M.J. MacLachlan, M. Jaroniec, G.A. Ozin, J. Am. Chem. Soc. **125**, 11662 (2003). doi:10.1021/ja036080z

228. W.H. Zhang, X.N. Zhang, L.X. Zhang, F. Schroeder, P. Harish, S. Hermes, J.L. Shi, R.A. Fischer, J. Mater. Chem. **17**, 4320 (2007). doi:10.1039/b708424b

229. O. Olkhovyk, S. Pikus, M. Jaroniec, J. Mater. Chem. **15**, 1517 (2005). doi:10.1039/b500058k

230. A.S. Chong, X.S. Zhao, Catal. Today **293**, 93 (2004)

231. M. Hartmann, Chem. Mater. **17**, 4577 (2005). doi:10.1021/cm0485658

232. S.Z. Qiao, H. Djojoputro, Q.H. Hu, G.Q. Lu, Prog. Solid State Chem. **34**, 249 (2006). doi:10.1016/j.progsolidstchem.2005.11.023

233. S.Z. Qiao, C.Z. Yu, W. Xing, Q.H. Hu, H. Djojoputro, G.Q. Lu, Chem. Mater. **17**, 6172 (2005). doi:10.1021/cm051735b

234. C.M. Li, J. Liu, X. Shi, J. Yang, Q.H. Yang, J. Phys. Chem. C **111**, 10948 (2007). doi:10.1021/jp071093a

235. A.M. Buswell, A.P.J. Middelberg, Biotechnol. Bioeng. **83**, 567 (2003). doi:10.1002/bit.10705

236. X.Q. Wang, D.N. Lu, R. Austin, A. Agarwal, L.J. Mueller, Z. Liu, J.Z. Wu, P.Y. Feng, Langmuir **23**, 5735 (2007). doi:10.1021/la063507h

237. F. Torney, B.G. Trewyn, V.S.Y. Lin, K. Wang, Nat. Nanotechnol. **2**, 295 (2007). doi:10.1038/nnano.2007.108

238. V. Rebbin, R. Schmidt, M. Froba, Angew. Chem. Int. Ed. **45**, 5210 (2006). doi:10.1002/anie.200504568

239. T. Martin, A. Galarneau, F. Di Renzo, D. Brunel, F. Fajula, S. Heinisch, G. Cretier, J.L. Rocca, Chem. Mater. **16**, 1725 (2004). doi:10.1021/cm030443c

240. C. Boissiere, M. Kummel, M. Persin, A. Larbot, E. Prouzet, Adv. Funct. Mater. **11**, 129 (2001). doi:10.1002/1616-3028(200104)11:2<129::AID-ADFM129>3.0.CO;2-W

241. T. Salesch, S. Bachmann, S. Brugger, R. Rabelo-Schaefer, K. Albert, S. Steinbrecher, E. Plies, A. Mehdi, C. Reye, R.J.P.

Corriu, E. Lindner, Adv. Funct. Mater. **12**, 134 (2002). doi:10.1002/1616-3028(20020201)12:2<134::AID-ADFM134>3.0.CO;2-A

242. D.J. Kim, J.S. Chung, W.S. Ahn, G.W. Kam, W.J. Cheong, Chem. Lett. **33**, 422 (2004). doi:10.1246/cl.2004.422

243. V. Rebbin, M. Jakubowski, S. PPtz, M. FrPba, Microporous Mesoporous Mater. **72**, 99 (2004). doi:10.1016/j.micromeso.2004.04.018

244. W.S. Ahn, K.K. Kang, K.Y. Kim, Catal. Lett. **72**, 229 (2001). doi:10.1023/A:1009084011436

245. Y.R. Ma, L.M. Qi, J.M. Ma, Y.Q. Wu, O. Liu, H.M. Cheng, Colloids Surf. A Physicochem. Eng. Asp. **229**, 1 (2003). doi:10.1016/j.colsurfa.2003.08.010

246. K.W. Gallis, J.T. Araujo, K.J. Duff, J.G. Moore, C.C. Landry, Adv. Mater. **11**, 1452 (1999). doi:10.1002/(SICI)1521-4095(199912)11:17<1452::AID-ADMA1452>3.0.CO;2-R

247. S.A. Trammell, M. Zeinali, B.J. Melde, P.T. Charles, F.L. Velez, M.A. Dinderman, A. Kusterbeck, M.A. Markowitz, Anal. Chem. **80**, 4627 (2008). doi:10.1021/ac702263t

248. N.A. Rakow, K.S. Suslick, Nature **406**, 710 (2000). doi:10.1038/35021028

249. A.A. Umar, M.M. Salleh, M. Yahaya, Sens. Actuators B Chem. **101**, 231 (2004). doi:10.1016/j.snb.2004.03.005

250. B. Johnson-White, M. Zeinali, K.M. Shaffer, C.H. Patterson Jr, P.T. Charles, M.A. Markowitz, Biosens. Bioelectron. **22**, 1154 (2007). doi:10.1016/j.bios.2006.07.040

251. M. Takezaki, T. Tominaga, J. Photochem. Photobiol. A **174**, 113 (2005). doi:10.1016/j.jphotochem.2005.02.013

252. S.S. Park, B. An, B.J. Melde, P.T. Charles, F.L. Velez, M.A. Dinderman, A. Kusterbeck, M.A. Markowitz, Microporous Mesoporous Mater. **111**, 367 (2008). doi:10.1016/j.micromeso.2007.08.012

253. R.D. Miller, Science **286**, 421 (1999). doi:10.1126/science.286.5439.421

254. S. Baskaran, J. Liu, K. Domansky, N. Kohler, X.H. Li, C. Coyle, G.E. Fryxell, S. Thevuthasan, R.E. Williford, Adv. Mater. **12**, 291 (2000). doi:10.1002/(SICI)1521-4095(200002)12:4<291::AID-ADMA291>3.0.CO;2-P

255. S. Yang, P.A. Mirau, C.S. Pai, O. Nalamasu, E. Reichmanis, J.C. Pai, Y.S. Obeng, J. Seputro, E.K. Lin, H.J. Lee, J.N. Sun, D.W. Gidley, Chem. Mater. **14**, 369 (2002). doi:10.1021/cm010690l

256. H.W. Ro, K.J. Kim, P. Theato, D.W. Gidley, D.Y. Yoon, Macromolecules **38**, 1031 (2005). doi:10.1021/ma048353w

257. B.D. Hatton, K. Landskron, W.J. Hunks, M.R. Bennett, D. Shukaris, D.D. Perovic, G.A. Ozin, Mater. Today **9**, 22 (2006). doi:10.1016/S1369-7021(06)71387-6

258. C.C. Yang, P.T. Wu, W.C. Chen, H.L. Chen, Polymer (Guildf) **45**, 5691 (2004). doi:10.1016/j.polymer.2004.05.071

259. B.D. Hatton, K. Landskron, W. Whitnall, D.D. Perovic, G.A. Ozin, Adv. Funct. Mater. **15**, 823 (2005). doi:10.1002/adfm.200400221